LA-11680-MS

c.3

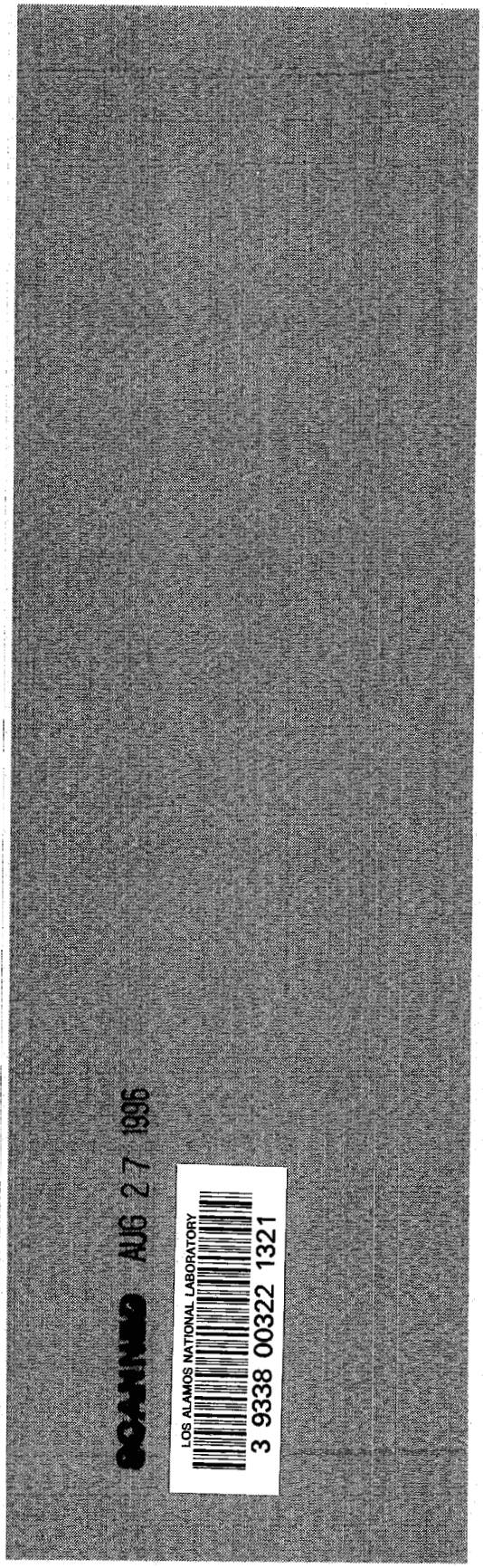

Quick, Reliable Estimates of High-Power Microwave Fluences: The SNEAKY-II Program

Los Alamos

Los Alamos National Laboratory is operated by the University of California for the United States Department of Energy under contract W-7405-ENG-36.

An Affirmative Action/Equal Opportunity Employer

LA-11680-MS

UC-905 and UC-910
Issued: January 1990

Quick, Reliable Estimates of High-Power Microwave Fluences: The SNEAKY-II Program

*T. W. Tunnell**
R. Roussel-Dupré

**EG&G, Energy Measurements, P. O. Box 809, Los Alamos, NM 87544.*

Los Alamos National Laboratory
Los Alamos, New Mexico 87545

QUICK, RELIABLE ESTIMATES OF HIGH-POWER MICROWAVE FLUENCES: THE SNEAKY-II PROGRAM

by

T. W. Tunnell and R. Roussel-Dupré

ABSTRACT

The propagation of high-power microwave pulses through the atmosphere is often modeled with time-dependent fluid or kinetic codes that require a fine mesh of range and time points. The computational time to run these codes precludes their use to determine the optimum pulse characteristics and propagation paths for delivery of a desired fluence to a specified target. In this work, a universal, parameterized scaling law for microwave-induced air breakdown is integrated into the SNEAKY model to produce a new microwave propagation code, SNEAKY-II. It estimates microwave fluences to within 1%–13% agreement with the more elaborate time-dependent fluid codes while running a hundred to several thousand times faster. The purpose of this report is to document the SNEAKY-II code, complete with benchmarking and specifications of the inherent limitations.

I. INTRODUCTION

During the avalanche process associated with microwave-induced air breakdown, the electron density $[n_e(t)]$ obeys an exponential growth,

$$n_e(t) = n_e(t=0)\exp\left[\int_0^t \nu_i dt'\right], \tag{1}$$

that is governed by the avalanche or ionization rate (ν_i). As the electron density grows, the current densities induced by the microwave pulse become large enough to ohmically dissipate the tail portion of the pulse over finite scale lengths. In the atmosphere, this effect occurs over distances $\sim$1 km, and the attenuation of the tail is sufficient to prevent further ionization. This phenomenon is known as tail erosion. If the microwave pulse is rapidly injected into an avalanche volume with sufficient energy, it is possible for ionization to proceed through the pulse until critical density ($\omega = \omega_p$, where ω is the angular frequency of the microwave pulse and ω_p is the electron plasma frequency) is achieved and reflection of the tail of the pulse occurs. This is the phenomenon of breakdown obtained in laboratory experiments. The fractional part of the original microwave fluence that is able to propagate through the atmosphere thus depends upon the effects of tail erosion and air breakdown.

The essential physics that defines the absorption and/or reflection of the incident microwave pulse involves the rapid formation and thermalization of an electron swarm. This problem has been treated in the past by means of detailed time-dependent solutions of either kinetic or fluid equations, including all the dominant electron-air interactions, in conjunction with Maxwell's equations to obtain the self-consistent evolution of the microwave pulse as well as the electron swarm. The equations constitute a nonlinear set that must be solved iteratively in time. In the special case when the root-mean-square (rms) electron temperature and mean velocity achieve a steady state, the ionization rate, momentum exchange rate (ν_m), and thermalization rate (ν_e) become constants that can be parameterized in terms of the rms electric field, microwave frequency, and atmospheric pressure. From these parameters it is possible to derive an attenuation scale length and estimate the amount of energy absorbed out of the microwave pulse. Assuming that the steady-state rates and corresponding attenuation scale lengths, whose functional dependence on the rms field is derived *a priori*, can be calculated from the *instantaneous* rms electric field in a time-varying pulse, we can determine the energy absorbed as a function of time through the pulse without having to resolve the microwave oscillations in time and without solving Maxwell's equations simultaneously as in the detailed kinetic and fluid treatments. This represents the SNEAKY concept, which has been implemented in several versions of the SNEAKY-II code. It offers a tremendous savings in computer time particularly for long, high-frequency pulses without sacrificing accuracy in the fluence levels and pulse shapes achieved after atmospheric propagation.

The implementation of the SNEAKY concept requires 1) a derivation of the attenuation scale length for microwaves in air and 2) a parameterization of the quantities that define this scale length in terms of an effective electric field strength divided by the atmospheric pressure. (The exact choice for this parameterization will be made clear later.) The former can be obtained analytically from the fluid equations for the electron swarm and Maxwell's equations, assuming a steady state, with the result

$$\Delta z = 2c\frac{(\nu^2+\omega^2)}{\omega_p^2\nu}, \tag{2}$$

where c is the vacuum speed of light, ν is the electron-neutral momentum exchange rate plus the ionization rate ($\nu_m + \nu_i$), ω is the angular frequency of the wave, and ω_p is the electron plasma frequency. The rate, ν, is a direct function of the electron energy that in turn depends on the electric-field strength, wave frequency, and atmospheric pressure. Similarly the plasma frequency is proportional to the electron density, which in turn is a direct function of the ionization rate [see Eq. (1)] integrated up to the time of interest into the microwave pulse. The ionization rate is a direct function of electron energy that ultimately depends on the electric field strength, wave frequency, and atmospheric pressure. A universal scaling law that parameterizes ν and ν_i in terms of an effective electric field divided by ν has been proposed and verified numerically (cf. Roussel-Dupré and Tunnell, 1989). The effective field is defined as

$$E_{\text{eff}} = \frac{E_{\text{rms}}}{\sqrt{(1+\omega^2/\nu^2)}}, \tag{3}$$

where E_{rms} is the instantaneous rms electric field. Given these scaling laws and the absorption scale length defined above, it is possible to obtain the attenuation of a microwave pulse propagating through the atmosphere. For the special case of a monopulse or broadband pulse, a different formulation for the effective field and attenuation scale length is used. It will be discussed in the following section.

In addition to attenuation, SNEAKY-II also treats the problem of ionospheric dispersion. This effect is particularly important for broad bandwidth signals such as monopulses. The treatment included in this code is approximate. It is assumed that the peak ionospheric plasma frequency is much less than the microwave frequencies of interest and that the frequency information contained in the initial pulse below approximately five times the peak plasma frequency is lost. The details of this analysis are discussed below.

The purpose of this report is to document the development of SNEAKY-II into a quick, reliable code to estimate the high-power microwave (HPM) fluence delivered on a target following atmospheric propagation. Section II describes the method of analysis used to derive and verify the universal scaling law. Section III discusses the numerical implementation of the SNEAKY concept, and Section IV describes the general flow of the program itself and presents input/output for a representative case. Section V documents the benchmarking of SNEAKY-II against fluid calculations and the fluid calculations against experimental measurements of air breakdown. Section VI gives a summary and a description of planned activities.

II. SCALING LAWS

A. Microwave Treatment

The time-dependent fluid analysis used to treat the problem of HPM propagation in air is simply a special case of the more general kinetic treatment in which the electron velocity distribution function is assumed to be a drifting Maxwellian defined in terms of three parameters: namely, density (n_e), mean velocity (v_0), and temperature (T_e). By taking appropriate moments of the Boltzmann equation, one obtains a set of equations that describe the temporal evolution of the electron gas. When electron spatial diffusion over the short time scales of interest and the ponderomotive force are neglected and the incident microwave pulse is assumed to be a plane-parallel wave, the fluid equations can be written

$$\frac{dn_e}{dt} = \nu_i(v_0, T_e)\, n_e, \tag{4}$$

$$\frac{dv_0}{dt} = \frac{-eE}{m_e} - [\nu_m(v_0, T_e) + \nu_i(v_0, T_e)]\, v_0, \text{ and} \tag{5}$$

$$\frac{dT_e}{dt} = \left[\frac{2\nu_e(v_0, T_e)}{3} - \nu_i(v_0, T_e)\right] T_e, \tag{6}$$

where t represents time, e is the absolute magnitude of the electron charge, m_e is the electron mass, and ν_c, ν_m, and ν_e are collision rates obtained by taking the first three moments (continuity, momentum conservation, and energy conservation) respectively of the Boltzmann collision integrals. The collision processes incorporated into our calculations include elastic, inelastic, and ionizing collisions of electrons with both N_2 and O_2. These equations are then solved in conjunction with Maxwell's equations to obtain a self-consistent result for the temporal evolution of the electromagnetic pulse as it propagates through the atmosphere. The Fluid Atmospheric Propagation (FLAP) code written for this purpose is described in detail in a report under preparation (Roussel-Dupré and Tunnell, 1989).

In deriving a scaling law to parameterize air breakdown, it is important to note that only the momentum equation contains the electric field explicitly. Because all other parameters depend on the electric field through v_0, a proper scaling of this quantity through the momentum equation should yield

the desired scaling law. In the special case where a constant electric field is applied to the plasma, the electron velocity in a steady state reduces to

$$v_0 = \frac{e}{m_e}\frac{E}{\nu}. \tag{7}$$

If we assume that ν can be approximated as a constant times the atmospheric pressure (e.g., $\nu = 5.3 \times 10^9 P/\text{torr}$, see Felsenthal and Proud, 1962), v_0 becomes a function of E/P only, and thus all parameters including the ionization rate can be written as functions of E/P. This fact combined with the solution to Eq. (4) [i.e., Eq. (1)] leads to the result in a steady state

$$P\tau = \frac{P}{\nu_i}\log_e \frac{n_e}{n_0}, \tag{8}$$

where τ is the time needed to achieve a density equal to n_e and n_0 is the initial electron density. If we choose n_e/n_0 as the density ratio needed to achieve breakdown and also realize that ν_i/P depends on E/P only, Eq. (8) yields a curve (E/P vs $P\tau$) for the threshold fields needed for breakdown given a square dc pulse of length τ. This formulation has been used extensively in the literature to present air breakdown thresholds obtained in dc experiments. A similar result can be derived for microwave breakdown. In this case the electric field strength oscillates in time, and the rms electron velocity can be written

$$(v_0)_{\text{rms}} = \frac{e}{m_e\nu}\frac{E_{\text{rms}}}{\sqrt{(1+\omega^2/\nu^2)}}, \tag{9}$$

where ω is the microwave angular frequency. Equating (7) and (9) yields the effective microwave field, Eq. (3), needed to produce the same mean electron velocity and presumably the same collision rates as those in the dc experiment. In this way a universal scaling law that allows one to derive breakdown thresholds for both microwave and dc fields from a single set of measurements is obtained. This formulation with ν equal to a constant times pressure (e.g., $\nu = 5.3 \times 10^9 p$) has also been used in the past to represent microwave breakdown thresholds. In some cases an attempt was made to include the effect of an energy-dependent ν (Felsenthal, 1966).

To test the accuracy of this scaling law the fluid code was run over a range of values of E_{eff}/P for a number of microwave frequencies and for dc electric fields. The steady-state results for $(v_0)_{\text{rms}}$, $\epsilon (= kT_e)$, ν_i/P, and ν/P are shown in Figs. 1a-d, whereas breakdown thresholds assuming that ν/P is a constant $\left(5.3 \times 10^9 s^{-1} torr^{-1}\right)$ and $n/n_0 = 1 \times 10^8$ are plotted in Fig. 1e. Substantial disagreement is obtained over a broad range of E_{eff}/P, suggesting that this scaling law is not appropriate. Indeed the assumption that ν/P is independent of the electric field is a poor one. The proper scaling law results in a plot of E_{eff}/ν vs $\nu\tau$ and requires that ν and all other collision rates be expressed as functions of E_{eff}/ν. Implementation of this new universal scaling law is less convenient, however, necessitating an iterative, tabular interpolation. The results shown in Figs. 2a–e substantiate the applicability of this new scaling.

B. Monopulse Treatment

For the special case of a broadband (fast-rise, short-duration) pulse, a somewhat different method of analysis is required. In this case the general time-dependent solution to the momentum equation is required to define an effective field. The general solution to Eq. (5) can be written

$$v_0(t) = \frac{e}{m_e} \int_0^t E(t') \exp\left[- \int_{t'}^t \nu(t'')dt'' \right] dt'. \tag{10}$$

Equating (10) and (7) yields the effective electric field needed to produce the same mean velocity and therefore the same collision rates as those in a dc experiment; namely,

$$E_{\text{eff}}(t) = \nu \int_0^t E(t') \exp\left[- \int_{t'}^t \nu(t'')dt'' \right] dt'. \tag{11}$$

Following the procedure outlined for the microwave and dc treatment described above, one can derive an expression for the attenuation scale length appropriate for this case with the result

$$\Delta z = \frac{2c\nu E}{\omega_p^2 E_{\text{eff}}}. \tag{12}$$

Equations (11) and (12) are then implemented in the same way as microwave propagation.

As noted in the Introduction, transionospheric propagation can become an issue for broadband pulses. The primary effect of a deterministic ionosphere is to disperse a pulse in time; i.e., the ionosphere introduces a frequency-dependent delay in the arrival of different frequency components. These delays are sufficiently large relative to the duration of pulses of interest (<1 μs) that the individual frequency components become resolvable in time, with the high frequencies arriving first. Near the cutoff frequency of the ionosphere (maximum plasma frequency), the time delays rapidly approach infinity. This fact sets an absolute lower limit on the frequency that can be modeled computationally, with a practical lower limit being somewhat above cutoff depending on the particular ionospheric model (i.e., total electron content). Two important scenarios develop from transionospheric propagation. One is propagation of the pulse through the ionosphere to a target in the lower atmosphere. In this case the pulse is significantly distorted in time by the ionosphere. The amount of absorption the pulse experiences in the lower atmosphere differs from what it would experience if it were launched below the ionosphere. For the other case, transionospheric propagation up to a target results in a distorted (chirped) pulse hitting the target.

In our analysis, transionospheric propagation is assumed to occur only at altitudes above 80 km and is accomplished by first integrating the electron density over the propagation path (= Total Electron Content, TEC), multiplying the transfer function of the ionosphere times the Fourier transform of the input pulse, and taking the inverse transform. To first order in the parameter ω_p^2/ω^2, where ω is an angular frequency component of the pulse and ω_p is the maximum plasma frequency over the propagation path, the ionospheric transfer function can be written

$$H(\omega) = \exp(-i\alpha/\omega) \tag{13}$$

with $\alpha = 2\pi e^2 N/m_e c$, N equal to the TEC, e the electron charge, and m_e the electron mass. Propagation is carried out over a frequency range determined by the frequency content of the pulse and the

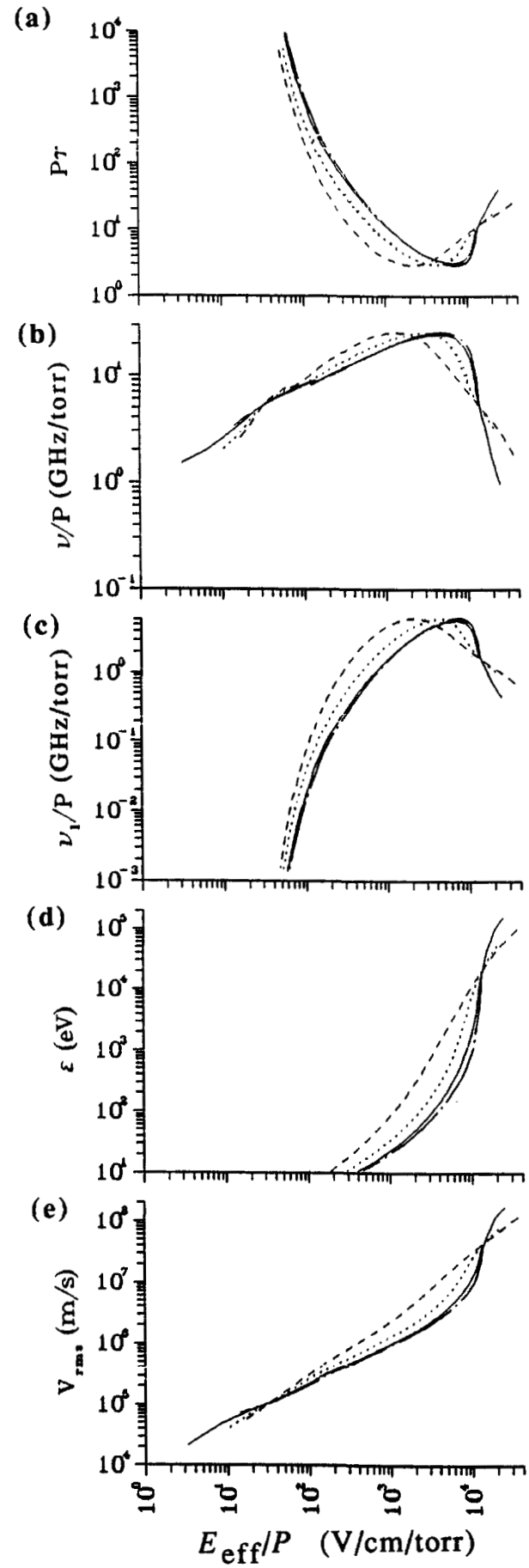

Figs. 1a–e. Steady-state results for the mean electron velocity (v_o), characteristic energy ($\epsilon = kT_e$), ionization rate divided by air pressure (ν_i/P), and momentum exchange rate divided by air pressure (ν/P) are plotted vs E_{eff}/P as shown in Figs. 1a–d, respectively. Breakdown thresholds assuming that ν/P is a constant ($= 5.3 \times 10^9 \text{s}^{-1}\ \text{torr}^{-1}$) and $n/n_o = 1 \times 10^8$ are plotted in Fig. 1e. The results presented in these figures were obtained with FLAP for the following frequencies: – – 3 GHz, · · · 10 GHz, – · – DC, — 1 GHz.

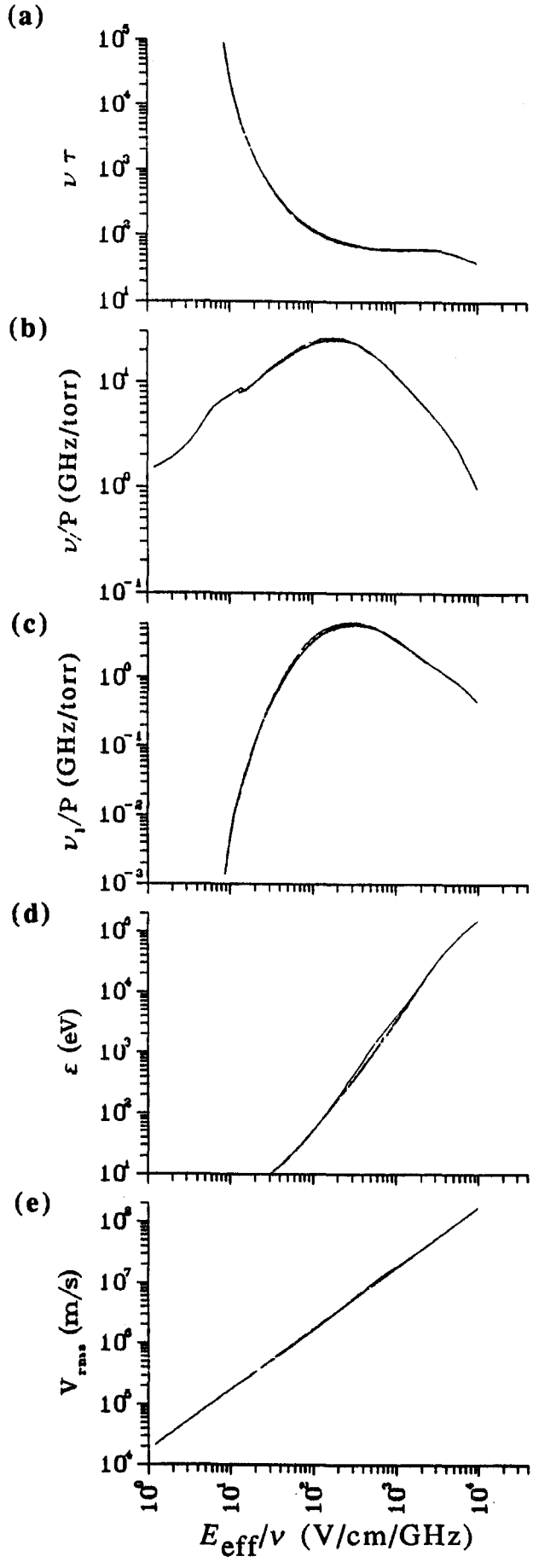

Figs. 2a–e. Steady-state results for the corresponding parameters in Figs. 1a–d are plotted vs E_{eff}/ν in Figs. 2a–d. Fig. 2e is a plot of breakdown thresholds in terms of the parameters E_{eff}/ν vs $\nu\tau$. These results are derived from the universal scaling law discussed in the text. Note that all of the curves for different frequencies are now aligned along a single curve.

maximum plasma frequency along the propagation path. All other frequencies are filtered out. The transionospheric pulse is then characterized in terms of rms envelope and a time-dependent frequency. Further propagation into the lower atmosphere, if necessary, is accomplished in the usual way with the scaling laws and attenuation scale lengths outlined above.

C. Implementation of Scaling Laws

The application of this analysis to microwave propagation is described in the Introduction. Basically, the fluid code (FLAP) is used to obtain a two-dimensional table of steady-state values for the collision rates as a function of rms electric field and microwave frequency, each divided by atmospheric pressure. Given an instantaneous value of the rms field, the microwave frequency for an arbitrary microwave pulse, and the atmospheric pressure, the table is then interpolated and corresponding electron density and attenuation scale length computed from Eqs. (1) and (2). The microwave pulse is then attenuated over a kilometer vertical distance at that instant in time and height, and the procedure is repeated with the attenuated pulse shape as a function of retarded time and altitude until propagation of the entire pulse through the atmosphere is complete. The use of steady-state parameters in a time-dependent problem forms the basis of the SNEAKY concept. Its accuracy has been checked *a posteriori* by comparing detailed fluid calculations for various pulse shapes, power levels, and antenna characteristics against the results of SNEAKY-II. The overall agreement for predictions of microwave fluence and propagation efficiency is in the range of 1%–13%. This result verifies the scaling law and method of analysis. It also suggests that measurements of steady-state collision rates can be substituted for the calculated values, insuring absolute accuracy in SNEAKY-II results.

III. DEVELOPMENT

A. Problem Description

HPM propagation through the atmosphere in the SNEAKY algorithm requires the specification of an antenna system for the delivery of microwaves and the temporal characteristics of the microwave pulse. The antenna is assumed to reside on a platform at a given altitude and to radiate into a solid angle defined by its diameter (D) and divergence angle (θ). The radiation is assumed to be uniform at any distance r from the antenna over an area

$$A = \pi(r + r_0)^2 \tan^2\theta, \tag{14}$$

where $r_0 = D/2\tan\theta$. Conservation of energy then requires that the power density vary with distance from the antenna as

$$P_r = P_0 \frac{r_0^2}{(r + r_0)^2}, \tag{15}$$

where P_0 is the power density at the antenna. This treatment is accurate in the far field but only approximate in the near field. Specific antenna designs that extend the near field or focus power into regions of potential air breakdown or tail erosion would have to be incorporated if accurate estimates of fluence and/or electron density profiles are necessary.

The input pulse is characterized in terms of the microwave frequency, total energy, and temporal length and shape. From this information the code generates the initial pulse at the platform in a format that utilizes only the envelope of the microwave electric field independent of the detailed oscillations.

B. Problem Setup

A typical application of SNEAKY-II is illustrated in Fig. 3. The triangle identifies the location of the microwave platform (at an altitude P_{alt}) while X represents the location of the target (at altitude T_{alt}). The slant range, R_N, is the total propagation distance between the platform and target. r_0 is the projection distance back to an equivalent point source as defined above, and the divergence angle θ describes the angular spread of the HPM radiation. Note that the platform is orientated facing the target. This picture defines the problem geometry.

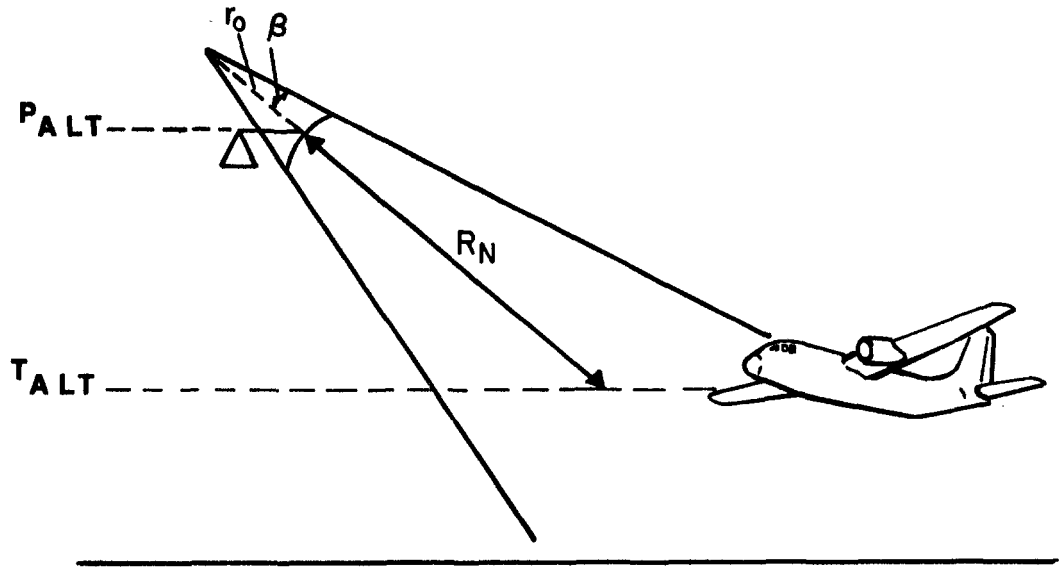

Fig. 3. The basic geometry employed in SNEAKY-II for a downward propagating pulse.

The general pulse characteristics are the microwave frequency (f), total energy (E_{tot}), pulse length (τ), and electric-field pulse

$$E(t) = A(t)\sin(\omega t), \tag{16}$$

where $A(t)$ is simply the envelope of the pulse. SNEAKY-II now defines the *instantaneous* rms electric field, $E_{\text{rms}}(t)$, to be

$$E^2_{\text{rms}}(t) = \frac{1}{\Delta t}\int_{t-\frac{\Delta t}{2}}^{t+\frac{\Delta t}{2}} A^2(t')\sin(\omega t')dt', \tag{17}$$

where (Δt) is taken to be a wave period. Assuming that $A(t)$ varies slowly over the time Δt, the result

$$E_{\text{rms}}(t) = \frac{A(t)}{\sqrt{2}} \tag{18}$$

is obtained. Because of its linear relationship with $A(t)$, the local rms field is also called the rms electric-field envelope, or simply rms envelope. At the platform, the rms envelope is further separated into an amplitude factor and shape factor:

$$E_{\text{rms}}(t) = E_{\text{max}}u(0,t). \tag{19}$$

The amplitude factor, E_{max}, is simply the peak value of the rms envelope, $E_{\text{rms}}(t)$. The shape factor, $u(0,t)$, is normalized so that it has a maximum value of 1 and is called the normalized envelope. The

0 argument in $u(0,t)$ identifies $u(0,t)$ as the normalized envelope at range R_0, or at the platform. In general, the normalized envelope changes shape in propagating from one range step to the next because of tail erosion, but this effect is discussed later under the attenuation subsection.

Currently, SNEAKY allows the user to select from four generic normalized envelopes or pulse shapes, namely, square, triangular, trapezoidal, and super-Gaussian. Samples of these normalized envelopes are shown in Figs. 4–7. In each case, τ is the total pulse length. In the triangular and trapezoidal pulse shapes, the envelope rises from 0 at time $t = 0$ to a maximum at time t_1, referred to as the rise time. The triangular pulse in Fig. 5 immediately begins to fall back toward zero after peaking. However, the trapezoidal pulse remains flat until time t_2, called the fall time point, when the pulse begins to fall back to zero. The super-Gaussian pulse takes on the form

$$u(0,t) = e^{-(\frac{t-t_0}{\Delta t})^N}, \tag{20}$$

where t_0 shifts the pulse to some appropriate delay, Δt is the $1/e$ half-width, and N is an even exponent that determines the flatness of the pulse as well as the rise and decay rates.

The peak rms electric field computed for each of the four pulse shapes from the total pulse energy, (E_{tot}), is

$$E_{\max} = \sqrt{\frac{377 f_l}{U^2}}, \tag{21}$$

where f_l is the total fluence at the platform. With r_a equal to the aperture radius, $f_l = E_{\text{tot}}/\pi r_a^2$. (U^2) is the integral

$$U^2 = \int_0^\tau u^2(0,t)dt. \tag{22}$$

Numerically, (U^2) is (τ), $(\tau/3)$, $[(\tau + t_1 - t_2)/3 + t_2 - t_1]$, and $2\Gamma(\frac{1}{N})\Delta t/N2^{\frac{1}{N}}$ for the square, triangular, trapezoidal, and super-Gaussian pulses respectively. It should be noted that SNEAKY-II can work with any pulse shape the user cares to generate.

C. Numerical Implementation of Scaling Law

Before (ν_i/P), (ν/P), (v_0), and (ϵ) can be scaled from (E_{eff}/ν), it must be possible to determine (E_{eff}/ν) for arbitrary (E_{rms}/P) and f/P. This task is complicated by the dependence of (E_{eff}) on (ν) as noted previously. The following logic describes how (E_{eff}/ν) can be determined for arbitrary (E_{rms}/P) and f/P.

First, assume that the set of input values $[E_1(n)/P$ for n=1,N] for the rms electric field to pressure ratios, used to generate the curves for the 1-GHz calculations shown in Figs. 2a–e, are arranged in ascending order so that $[E_1(n+1)/P \geq E_1(n)/P]$. Also assume that the collision rate coefficients $[\nu_1(n)/P]$ for the 1-GHz calculations are ordered so that $[\nu_1(n)/P]$ is the value of the rate coefficient (ν/P) that was computed for an input rms electric field to pressure ratio of $E_1(n)/P$. The quantity E_{eff}/ν for these data sets can then be expressed as

$$\frac{E_{\text{eff}}(n)}{\nu(n)} = \frac{E_1(n)}{P} \frac{1}{\sqrt{\left[\frac{\nu(n)}{P}\right]^2 + \left(\frac{\omega_1}{P}\right)^2}}, \tag{23}$$

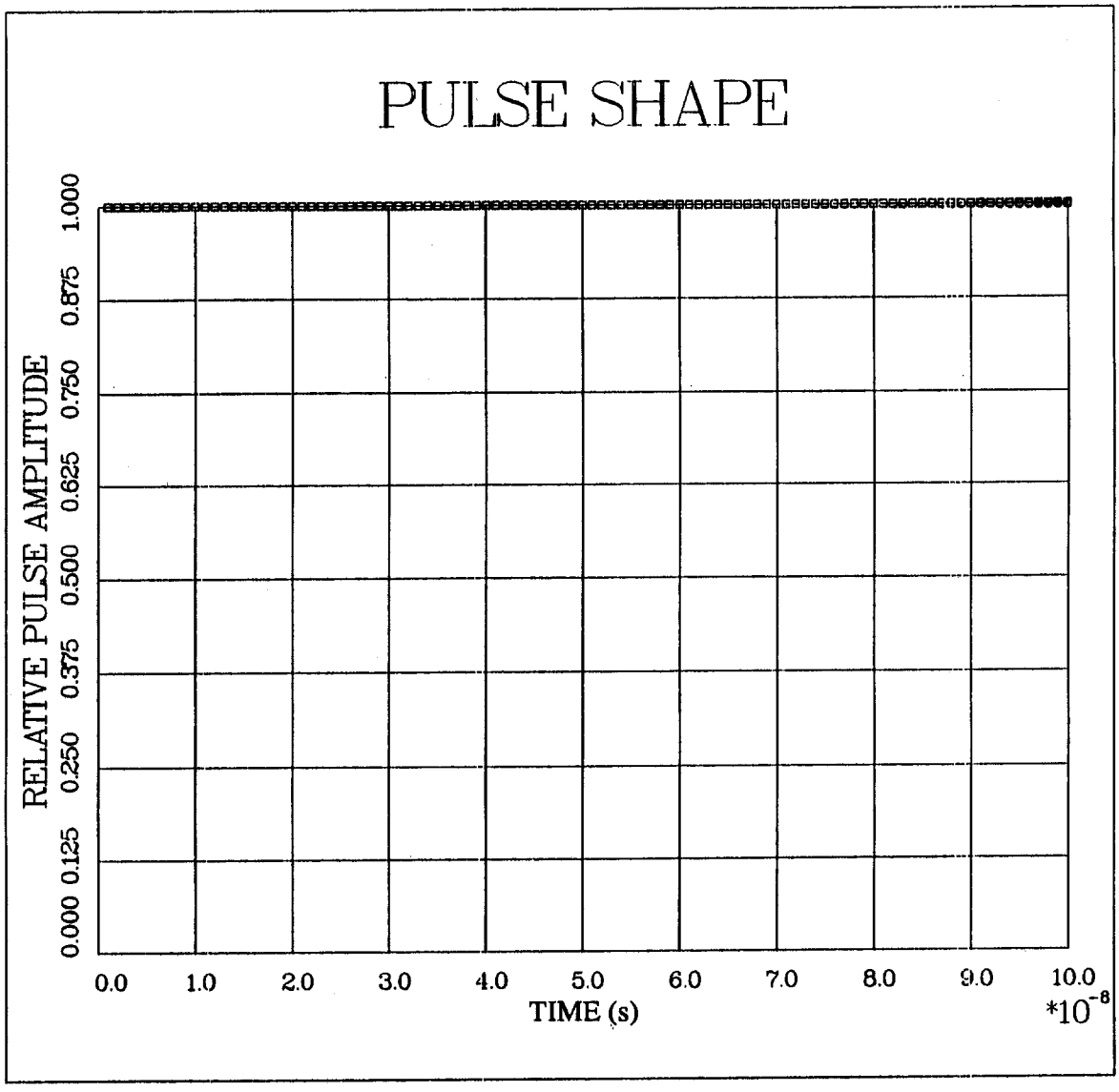

Fig. 4. Square pulse.

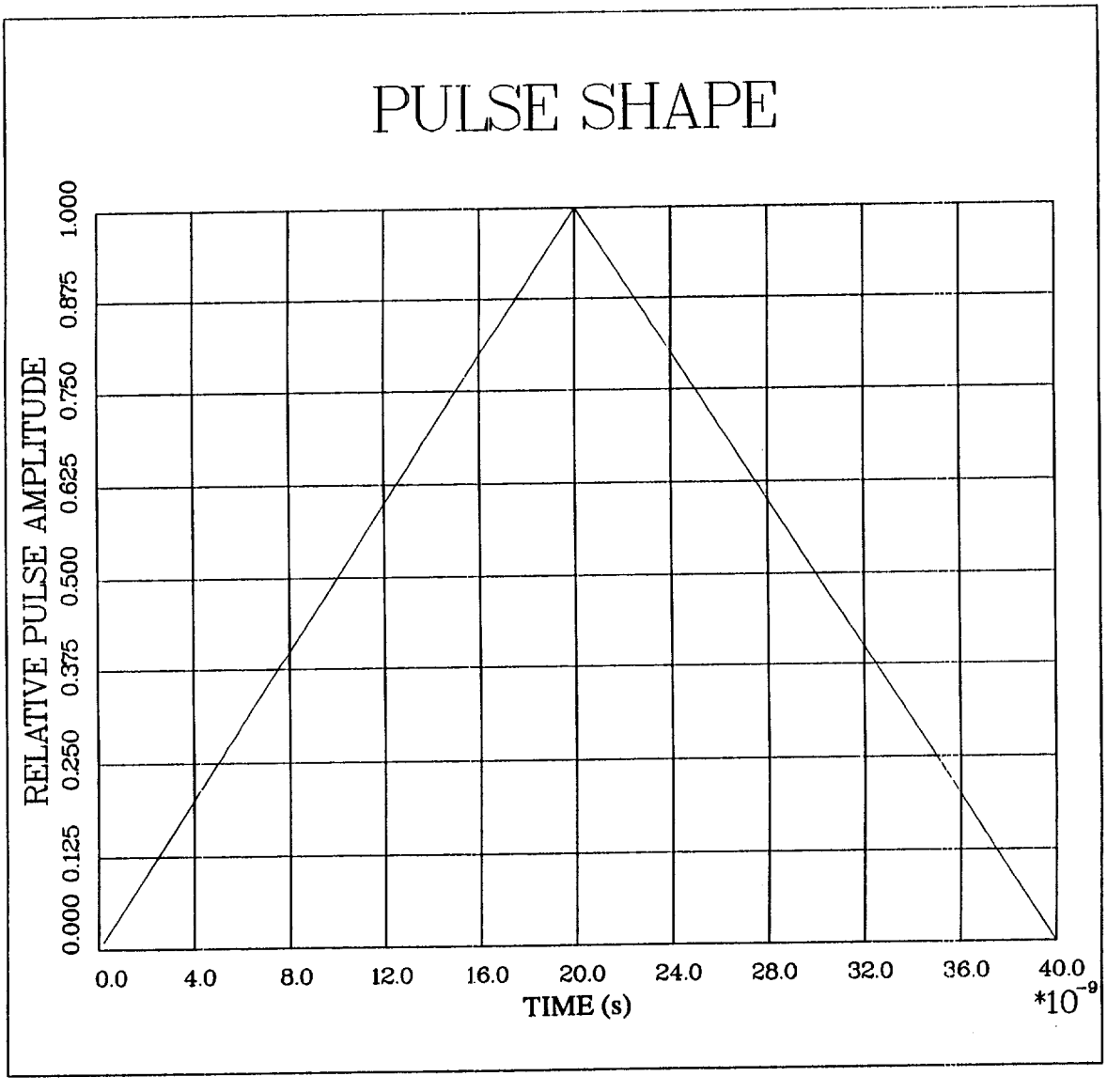

Fig. 5. Triangular pulse.

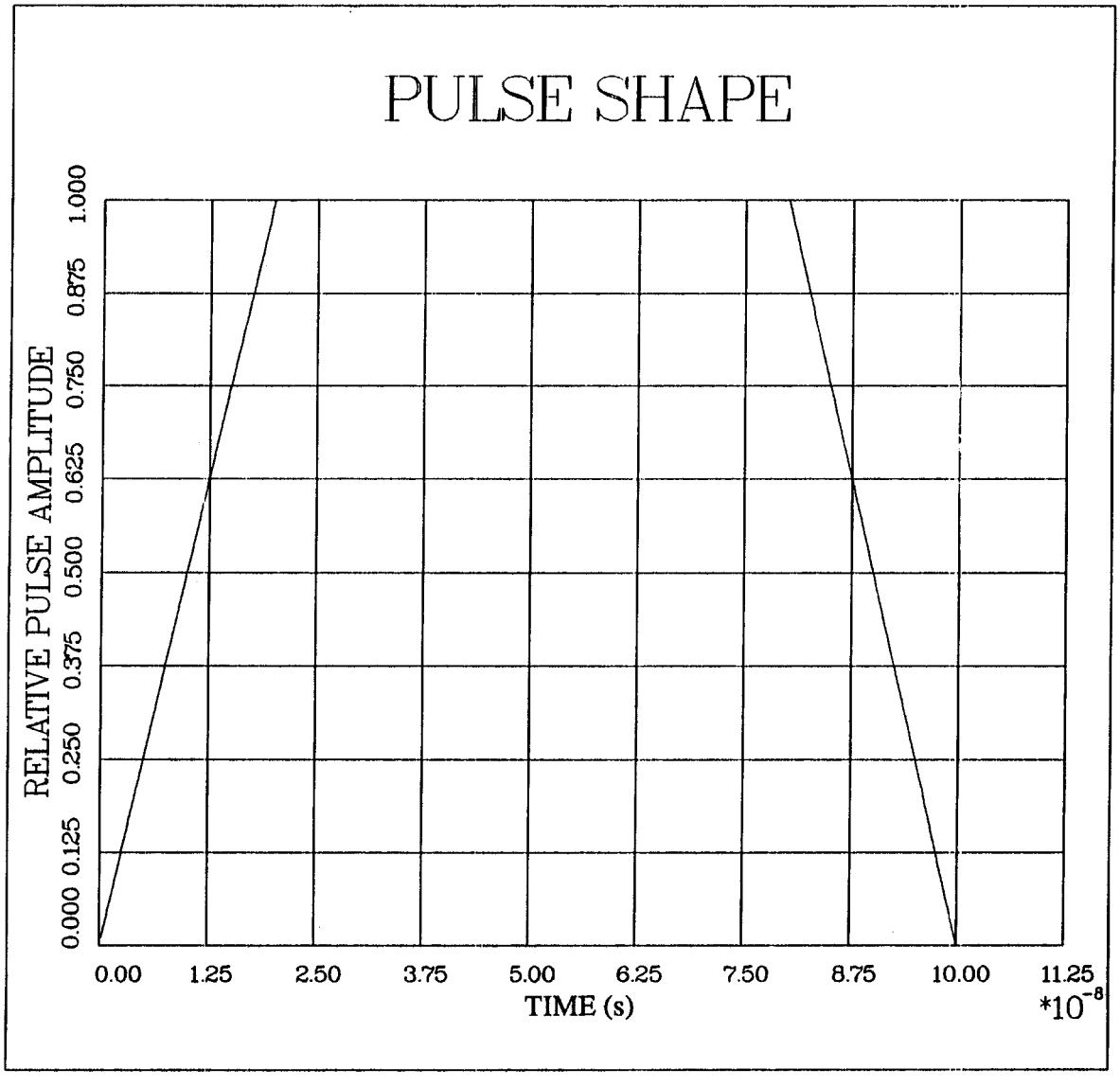

Fig. 6. Trapezoidal pulse.

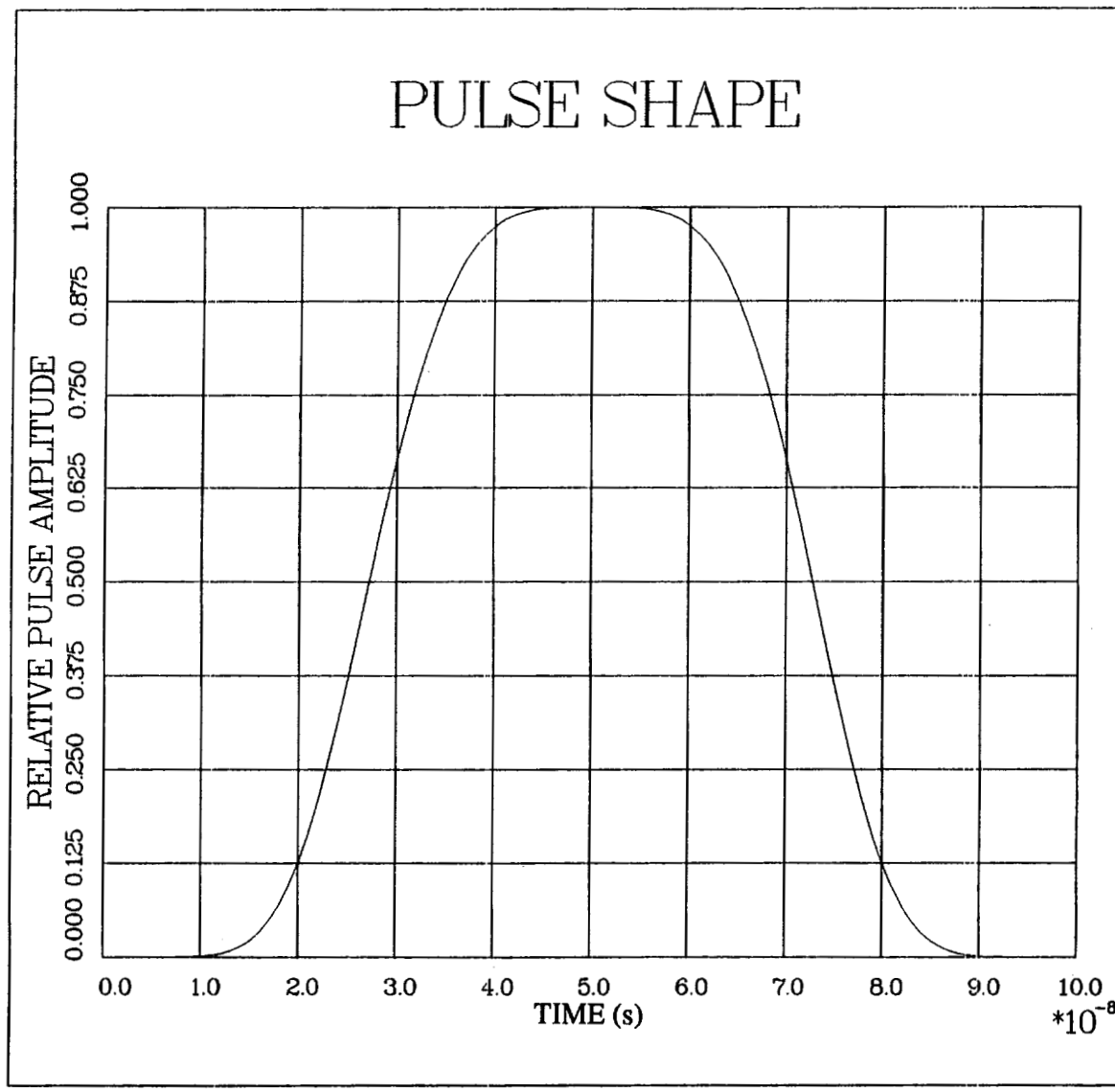

Fig. 7. Super-Gaussian pulse.

where $\omega_1 = 2\pi$ times 1 GHz.

Now consider a microwave pulse of arbitrary frequency f and a point of time when the rms envelope has a local value of $E_{\rm rms}(t)$. Let P be the pressure of the air through which the pulse is propagating, and define the *instantaneous* $E_{\rm eff}/\nu$ $[E_{\rm eff}(t,n)/\nu(n)]$ for the pulse at this time as

$$\frac{E_{\rm eff}(t,n)}{\nu(n)} = \frac{E_{\rm rms}(t)}{P} \frac{1}{\sqrt{\left[\frac{\nu(n)}{P}\right]^2 + (\frac{\omega}{P})^2}}. \tag{24}$$

One then searches the table of values generated for $E_1(n)/P$ and ω_1/P for the combination of $E_{\rm eff}(n)/\nu(n)$ and $\nu(n)$ that yields an equivalence between Eqs. (23) and (24). In general, because of the limited data set for $E_1(n)/P$ and $\nu(n)$, no $E_1(n)/P$ and $\nu(n)/P$ data pair will exist in which $E_{\rm eff}(t,n)/\nu(n) = E_{\rm eff}(n)/\nu(n)$. However, because $E_{\rm eff}/\nu$ is a monotonically increasing function of $E_{\rm rms}/P$, a value of n will exist for which

$$\frac{E_{\rm eff}(n)}{\nu(n)} \leq \frac{E_{\rm eff}(t,n)}{\nu(n)} \tag{25}$$

and

$$\frac{E_{\rm eff}(n+1)}{\nu(n+1)} \geq \frac{E_{\rm eff}(t,n+1)}{\nu(n+1)}, \tag{26}$$

unless $E_{\rm rms}(t)/P$ is too large [Inequality (25) always applies] or too small [Inequality (26) always applies].

For implementation into a FORTRAN routine the Inequalities (25) and (26) can be better expressed in terms of the difference $D(n)$ defined as

$$D(n) = \left[\frac{E_1(n)}{P}\right]^2 - \left(\frac{E_{\rm rms}}{P}\right)^2 \frac{1 + \left[\frac{\omega_1}{\nu(n)}\right]^2}{1 + \left[\frac{\omega}{\nu(n)}\right]^2} \tag{27}$$

with $D(n) \leq 0$ and $D(n+1) \geq 0$. This is achieved by requiring $D(n)D(n+1) \leq 0$. The logic is then to compute the difference as defined in Eq. (27) until the product of two successive values $[D(n)D(n+1)]$ is found to be negative. When this condition is met, the true $E_{\rm eff}/\nu$ must necessarily lie between $E_{\rm eff}(n)/\nu(n)$ and $E_{\rm eff}(n+1)/\nu(n)$, and it becomes a matter of interpolating between the two values to determine an approximate $E_{\rm eff}/\nu$.

The interpolation procedure consists of a number of steps. First, a simple linear interpolation is performed between the $E_1(n)/P$ data points to determine the value of E/P (E_i/P) at which the difference in Eq. (27) vanishes;

$$\frac{E_i}{P} = \frac{D(n+1)\frac{E_1(n)}{P} - D(n)\frac{E_1(n+1)}{P}}{D(n+1) - D(n)}. \tag{28}$$

A simple linear interpolation is used because $E_{\rm eff}/\nu$ is approximately linear over small ranges of the rms field strength. A second linear interpolation is performed to obtain the interpolated $E_{\rm eff}/\nu$:

$$\frac{E_{\rm eff}}{\nu} = \frac{E_{\rm eff}(n)}{\nu(n)} + \left[\frac{E_{\rm eff}(n+1)}{\nu(n+1)} - \frac{E_{\rm eff}(n)}{\nu(n)}\right] C_e, \tag{29}$$

where

$$C_e = \frac{\frac{E_i}{P} - \frac{E_1(n)}{P}}{\frac{E_1(n+1)}{P} - \frac{E_1(n)}{P}}. \tag{30}$$

Note that the pressure P divides out in the expression for C_e. Experience has shown that values of ν_i/P, ν/P, ϵ, and $\nu\tau$ are best obtained via a log-log interpolation:

$$\log\frac{\nu_i}{P} = \log\frac{\nu_i(n)}{P} + A_e \log\frac{\nu_i(n+1)}{P}\frac{P}{\nu_i(n)}, \tag{31}$$

$$\log\frac{\nu}{P} = \log\frac{\nu(n)}{P} + A_e \log\frac{\nu(n+1)}{P}\frac{P}{\nu(n)}, \tag{32}$$

$$\log\epsilon = \log\epsilon(n) + A_e \log\frac{\epsilon(n+1)}{\epsilon(n)}, \tag{33}$$

and

$$\log\nu\tau = \log\nu\tau(n) + A_e \log\frac{\nu\tau(n+1)}{\nu\tau(n)}, \tag{34}$$

where

$$A_e = \frac{\log\frac{E_{\text{eff}}}{\nu} - \log\frac{E_{\text{eff}}(n)}{\nu(n)}}{\log\frac{E_{\text{eff}}(n+1)}{\nu(n+1)} - \log\frac{E_{\text{eff}}(n)}{\nu(n)}}. \tag{35}$$

D. Attenuation

As the pulse propagates through the atmosphere, it suffers a geometric spreading loss and attenuation due to tail erosion. The geometric spreading loss is a function of range only and calculated for the n^{th} range step, R_n, as $E_h(n) = R_0/R_n$. Because tail erosion is both a range and a time-dependent effect and because our desire is to represent pulse shape distortion in terms of a unit-normalized-shape function, it is convenient to express the rms envelope at range R_n as

$$E_{\text{rms}}(n,t) = E_{\text{max}} E_h(n) E_{\text{af}}(n) u(n,t). \tag{36}$$

This procedure has the advantage of separating the rms envelope into the initial peak value (E_{max}), a spreading loss term [$E_h(n) = R_0/R_n$], a term [$E_{\text{af}}(n)$] that represents the fractional loss in the peak field due to tail erosion, and a unit-normalized envelope $u(n,t)$ that immediately identifies pulse shape distortion due to tail erosion.

In propagating to the next range, the pulse suffers additional geometric spreading loss and attenuation due to tail erosion. The additional geometric spreading loss is R_n/R_{n+1} for a total spherical spreading loss of $E_h(n+1) = R_0/R_{n+1}$. The additional attenuation due to tail erosion is a function of time, $\alpha(t)$, and changes the relative shape of the normalized envelope from $u(n,t)$ to $\alpha(t)u(n,t)$. If we account for both the spherical spreading loss and the tail erosion, the rms envelope at range R_{n+1} is then

$$E_{\text{rms}}(n+1,t) = E_{\text{max}} E_h(n+1) E_{\text{af}}(n) \alpha(t) u(n,t), \tag{37}$$

where we have used the fact that $E_{\text{af}}(n+1)u(n+1,t) = E_{\text{af}}(n)\alpha(t)u(n,t)$. The quantity $\alpha(t)$ is simply the time-dependent exponential attenuation factor

$$\alpha(t) = e^{-\frac{\Delta R}{\Delta s(t)}}, \tag{38}$$

where ΔR is a range step, $\Delta z(t)$ is the attenuation scale length given by Eq. (2) or Eq. (12) and where the rate parameters that define $\Delta z(t)$ are obtained by the procedure outlined below. Given that $u(n+1,t)$ is proportional to $\alpha(t)u(n,t)$, and that the maximum value of $u(n+1,t)$ is unity as required by the definition of normalized envelope, it follows that the constant of proportionality must be the reciprocal $[1/u_{\max}(n)]$ of the the maximum value $[u_{\max}(n)]$ of $\alpha(t)u(n,t)$. Thus

$$u(n+1,t) = \alpha(t)\frac{u(n,t)}{u_{\max}(n)}, \tag{39}$$

and consequently,

$$E_{\text{af}}(n+1) = E_{\text{af}}(n)u_{\max}(n). \tag{40}$$

In this simple manner, tail erosion is added to the pulse as it propagates through the atmosphere from the platform to the target. With the previous logic to determine E_{eff}/ν and the rate coefficients, ν_i/P and ν/P, for arbitrary $E_{\text{rms}}(t)/P$ and f/P, the attenuation $\alpha(t)$ can easily be calculated as is discussed next.

From the scaling law discussed in the previous subsection, it is possible to compute $\nu(t)/P$ and $\nu_i(t)/P$ from $E_{\text{rms}}(t)$, f, and P and, subsequently, $\nu(t)$ and $\nu_i(t)$. From the values for $\nu(t)$ and $\nu_i(t)$, one could obtain corresponding averaged values to compute the attenuation $\alpha(t)$ over the time interval t to $t+\Delta t$. But this is not done; rather, SNEAKY-II adheres to the principle of a local rms electric field. That is, instead of averaging the rates over the time interval, SNEAKY-II obtains the local rms electric field over the time interval as

$$\begin{aligned} E_{\text{rms}} &= E_{\max}E_h(n)E_{\text{af}}(n)\sqrt{\int_t^{t+\Delta t} u^2(n,t')\frac{dt'}{\Delta t}} \\ &\sim E_{\max}E_h(n)E_{\text{af}}(n)\sqrt{\frac{u^2(n,t)+u(n,t)u(n,t+\Delta t)+u^2(n,t+\Delta t)}{3}}, \end{aligned} \tag{41}$$

where a linear interpolation has been assumed between $u(n,t)$ and $u(n,t+\Delta t)$. The corresponding values for ν/P and ν_i/P are then computed from the scaling law using E_{rms} as the appropriate local rms electric field. In general, the range step ΔR in Eq. (38) is chosen so that $\alpha(t=0) \geq 0.99$. This procedure may require dividing ΔR into a number of smaller range steps and does not present any numerical difficulties.

E. Dynamic Time Scale

The scaling feature of SNEAKY assumes that the details of the electric field can be adequately described by a local rms electric field over an appropriate time interval. Longer time intervals are applicable when the rms electric field changes slowly, and shorter time intervals are required when the rms electric field is changing more rapidly in order to maintain an acceptable level of accuracy. A high sampling rate is therefore a requirement for a desired level of accuracy. But the greater number of samples involved with higher sampling rates compromises SNEAKY's speed advantage. The dynamic time scale feature that was developed for the SNEAKY-II code samples the rms envelope so that two successive samples differ by exactly 1% of the peak value, exclusive of the end points. In terms of the normalized envelope, this sampling feature can be expressed as

$$\mid u(n,t_k) - u(n,t_{k+1}) \mid \leq 0.01 \tag{42}$$

for $k = 2, 3, 4, \ldots M-1$ where M is the total number of data samples of the normalized envelope.

Primarily for ease of development into a FORTRAN routine, the additional criteria that $u(n, t_k)$ be an integral multiple of 0.01 [$u(n, t_k) = 0.00, 0.01, 0.02, \ldots,$ or 1.00] was imposed for $k = 2, 3, 4, \ldots M-1$.

The analytical nature (i.e., square, triangular, trapezoidal, super-Gaussian) of the initial pulse shapes makes it an easy matter to generate the pulse at the platform with the appropriate sampling. Initially, the square pulse is sampled uniformly as

$$u(0, t_k) = 1.0, \tag{43}$$

where $t_k = (k-1)t/100$ for $k = 1, 2, 3, \ldots 101$. The sampling of the triangular pulse is separated into two regimes, namely the rise ($t_k \leq t_1$) and the fall ($t_k \geq t_1$). During the rise, the normalized envelope is sampled as

$$u(0, t_k) = \frac{k-1}{100} \quad \text{for} \quad t_k = \frac{(k-1)t_1}{100}, \tag{44}$$

with $k = 1$ to 101. Note that 101 points describe the rise. For the fall, the points are selected as

$$u(0, t_k) = 1 - \frac{k-101}{100} \quad \text{for} \quad t_k = t_1 + \frac{(k-101)(\tau - t_1)}{100}, \tag{45}$$

with $k = 101$ to 201. An additional 100 points are used for the fall of the pulse (the 101^{st} point is the vertex of the triangle and is common to both the rise and the fall) for a total of 201 points. In a similar manner, the trapezoidal pulse is divided into three regimes: the rise ($t_k \leq t_1$), the plateau ($t_1 \leq t_k \leq t_2$), and the fall ($t_k \geq t_2$). As in the triangular pulse, the rise is sampled as

$$u(0, t_k) = \frac{k-1}{100} \quad \text{for} \quad t_k = \frac{(k-1)t_1}{100}. \tag{46}$$

Fifty points are used to describe the plateau portion:

$$u(0, t_k) = 1 \quad \text{for} \quad t_k = t_1 + \frac{(k-101)(t_2 - t_1)}{50}. \tag{47}$$

A final 100 points are used in the fall of the pulse:

$$u(0, t_k) = 1 - \frac{k-1}{100} \quad \text{for} \quad t_k = \frac{(k-151)(\tau - t_2)}{100}. \tag{48}$$

The initial super-Gaussian pulse is generated in a way similar to that of the trapezoidal pulse, which for the first 100 points results in

$$u(0, t_k) = u(0, 0) + \frac{k-1}{100} \quad \text{for} \quad t_k = t_0 + \left(\log_e \frac{100}{k-1}\right)^{\frac{1}{N}} \Delta t \tag{49}$$

for $0 \leq t_k \leq t_1$, $k > 1$ and $u(0,0)$ equal to the super-Gaussian evaluated at $t = 0 (k = 1)$. For the next 50 points we have

$$u(0, t_k) = e^{-(\frac{t_k - t_0}{\Delta t})^N} \quad \text{for} \quad t_k = t_1 + \frac{(k-101)(t_2 - t_1)}{50} \tag{50}$$

and for the last 100 points

$$u(0,t_k) = u(0,0) - \frac{k-150}{100} \quad \text{for} \quad t_k = t_2 + (\log_e \frac{100}{251-k})^{\frac{1}{\nu}} \Delta t. \tag{51}$$

To insure that the super-Gaussian pulse is continuous, has a small magnitude at the origin, and has the specified pulse length, the user must choose t_0 and τ such that $t_0/\tau, (\tau - t_0)/\Delta t > 3$. Note that the flat portions of the square, trapezoidal, and super-Gaussian pulses are initially oversampled.

As tail erosion modifies the pulse shape from one range step point to the next, it becomes necessary to resample with a new set of time points, t'_m, so that $u(n+1,t'_m)$ satisfies the dynamic time scale criteria outlined above. The resampling is performed by computing a temporary normalized envelope $u_T(t_k)$ as

$$u_T(t_k) = \alpha(t_k)\frac{u(n,t_k)}{u_{\max}(n)} \tag{52}$$

for $k = 1,2,3,...M$ and interpolation between the data pairs $(u_T(t_k),t_k)$ to determine t'_m $m = 2,3,4...M'-1$ so that $u(n+1,t'_m)$ will satisfy the dynamic time scale criteria. The first resampled time point t'_1 is then defaulted to 0 so that $u(n+1,t'_1) = u_T(t_1)$. The second resampled time point t'_2 is determined via a simple linear interpolation. To describe the strong time dependence (at least exponential in time), a log-log interpolation is used to resample the later time points $(t'_m, m \geq 3)$.

To meet the dynamic time scale sampling requirements, $u(n+1,t'_2)$ is chosen so that $u(n+1,t'_2)$ is an integral multiple of 0.01 and so that $\|u(n+1,t'_1) - u(n+1,t'_2)\| \leq 0.01$. Selecting $u(n+1,t'_2) = (N_I + 1/2 \pm 1/2)0.01$ where (N_I) is the integer portion of $u_T(t_1)/0.01$ satisfies these requirements. If $u_T(t_k)$ rises above $0.01(N_I+1)$ before it falls below $0.01N_I$, then $u(n+1,t'_2)$ is defined as $0.01(N_I+1)$. Otherwise, $u(n+1,t'_2)$ is selected as $0.01N_I$. The resampled time point t'_2 is evaluated numerically as the linear interpolation

$$t'_2 = t'_1 + \frac{t_2 - t_1}{u_T(t_2) - u_T(t_1)}[u(n+1,t'_2) - u_T(t_1)], \tag{53}$$

where t_2 is the first time point at which $u_T(t_k)$ either rises above $0.01(N_I+1)$ or falls below $0.01N_I$.

The resampled time points $t'_m, m = 3,4,5,...M'$ are selected next via the log-log interpolation

$$\log t'_m = \log t_{k-1} + \frac{\log t_k - \log t_{k-1}}{\log u_T(t_k) - \log u_T(t_{k-1})}[\log u(n+1,t'_m) - \log u_T(t_{k-1})], \tag{54}$$

where $u(n+1,t'_m) = u(n+1,t'_{m-1}) \pm 0.01$. t_k is the first time point $> t'_{m-1}$ such that $u_T(t_k) > u(n+1,t'_{m-1}) + 0.01$ or $< u(n+1,t'_{m-1}) - 0.01$.

F. Output

At each altitude step, SNEAKY-II computes a fluence, efficiency, average attenuation, average collision rates, average effective electric field, and the decay times, where average refers in general to some weighted integral in time. This subsection defines these quantities and gives the details of how they are calculated.

1. Fluence

The fluence is computed as

$$f_l = \frac{c}{4\pi}\int_0^\tau E^2(t)dt \tag{55}$$

$$= \frac{c}{4\pi}[E_{\max}E_h(n)E_{af}(n)]^2\int_0^\tau u^2(n,t)dt, \tag{56}$$

where the integral of $u^2(n,t)$ is approximated as the sum

$$\int_0^\tau u^2(n,t)dt \sim \Sigma\frac{[u^2(n,t_k)+u(n,t_k)u(n,t_{k+1})+u^2(n,t_{k+1})]}{3}(t_{k+1}-t_k). \tag{57}$$

2. Efficiency

The total energy, $E_{tot}(n)$, that propagates to range R_n is then $f_l = \pi[R_n tan(\theta)]^2$. The efficiency, ϵ, is simply the ratio of $E_{tot}(n)$ and $E_{tot}(0)$:

$$\epsilon = \frac{E_{tot}(n)}{E_{tot}(0)}. \tag{58}$$

3. 90%, 50%, and 10% Decay Times for a Square Pulse

The 90%, 50%, and 10% decay times ($t_{90\%}$, $t_{50\%}$, and $t_{10\%}$, respectively) are defined as the time that the normalized envelope of an initially square pulse has decayed to 0.90, 0.50, and 0.10. That is,

$$u(n,t_{90\%}) = 0.90 \tag{59}$$

$$u(n,t_{50\%}) = 0.50 \tag{60}$$

$$u(n,t_{10\%}) = 0.10 \tag{61}$$

These time points really have meaning only for an initially square, or near square, pulse. They are computed to help facilitate the user's understanding of how tail erosion is changing the pulse shape along the propagation path.

4. Average Rate Coefficients

The average rate coefficients, $< \nu/P >$ and $< \nu_i/P >$, are calculated as straight time averages:

$$< \frac{\nu}{P} > = \frac{1}{\tau}\int_0^\tau \frac{\nu}{P}dt \tag{62}$$

$$< \frac{\nu_i}{P} > = \frac{1}{\tau}\int_0^\tau \frac{\nu_i}{P}dt \tag{63}$$

5. Average Attenuation

The average attenuation, $< 1/\Delta z >$, is computed as the density weighted time average

$$< \frac{1}{\Delta z} >= \frac{\int_0^\tau \frac{1}{\Delta z(t')} n_e(t')dt'}{\int_0^\tau n_e(t')dt'}. \tag{64}$$

6. Trajectory in E_{eff}/ν vs $\nu\tau$ Space

As noted previously, it is possible to define breakdown as the time necessary to achieve a specified electron density for a given applied electric field, and thus breakdown thresholds can be plotted parameterically as E_{eff}/ν vs $\nu\tau$. In this same space one can identify a threshold curve for tail erosion by simply calculating the plasma density for which a given attenuation scale length is obtained. This calculation leads to a curve parallel to the breakdown curve but displaced to smaller values of $\nu\tau$, as lower densities are needed for attenuation than for breakdown. It is then possible to plot a third curve that represents the trajectory of the microwave pulse through this space, yielding detailed information about the plasma swarm and attenuation as the pulse propagates through the atmosphere. Given the input data set described above, it is a trivial matter to generate the breakdown and tail erosion threshold curves. The trajectory of the microwave pulse is generated by calculating a density-weighted (in time) attenuation scale length at each altitude and scaling $\nu\tau$ relative to the 1 km (attenuation scale length) tail erosion curve. Thus, $\nu\tau_{\text{pulse}} = \nu\tau_{\text{tail-erosion}}(1 + \log_e \frac{10^5}{\Delta z} / \log_e 10^4)$.

IV. PROGRAM FLOW AND REPRESENTATIVE I/O

The SNEAKY-II program is written in standard FORTRAN 77 and presently runs on a VAX with a VMS operating system. The input/output takes the form of standard formatted files along with graphics output obtained with the use of @DISSPLA. The code starts by initializing various constants and variables and proceeds by asking the user to specify an input file (NAME.DAT, where NAME is specified by the user). If no file is given then a default set of parameters is supplied. A sample input file is shown in Table I. At this point the user has the option of changing any of the parameters and writing the new set to a specified file. The input values are also written to an output file (NAME.OUT) so that the user has a record of the particular case being run, along with the propagation results. Depending on the platform and target altitudes and on the direction of propagation (up through the atmosphere or down), the code decides whether or not to compute the total electron content (in subroutine CTEC) and over what altitude range. SNEAKY-II then generates the input pulse (in subroutine PULSER) based on the specified pulse parameters. If propagation is downward and the platform is above 80 km, then ionospheric propagation is carried out (in subroutine CDISP) to the target altitude or 80 km, whichever is greater. The output from CDISP consists of the dispersed pulse envelope and an array containing the corresponding frequency as a function of time. These arrays are passed through an interpolation routine (subroutine TIMER) to obtain a new pulse such that the amplitude changes by no more than 1% of the maximum value in any given time step.

At this point the code is prepared to carry out propagation between 0 and 100 km. Absorption due to air breakdown is assumed to occur only in this altitude range, and this calculation is carried out to or from 100 km whether or not transionospheric propagation has been computed to 80 km. In other

Table I
SNEAKY-II Input Parameters

1.	Aperture Radius (cm)	=	56.4
2.	Divergence Half-Angle (deg)	=	181
3.	Platform Altitude (km)	=	0
4.	Target Altitude (km)	=	100
5.	Slant Range (km)	=	100
6.	Total Energy in Pulse (J)	=	10
7.	Pulse Length (s)	=	3.00E-09
8.	File Name for this Case	=	SD1
9.	Microwave Frequency (GHz)	=	1.00
10.	Pulse Type	=	1
11.	Receiver Antenna Gain	=	1.00
12.	Receiver Frequency	=	2.86

words the processes of absorption and dispersion are assumed to be independent in this approximate analysis. The amount of energy absorbed out of the pulse at each altitude step (= 1 km) as described in previous sections is computed in three subroutines: STEPPER, SHAPER, and SUMMER. STEPPER determines the minimum absorption scale length to be expected at a given altitude on the basis of the pulse parameters, and it subdivides the kilometer altitude step into smaller steps such that no more than 1% attenuation occurs in a substep. STEPPER then calls SHAPER and TIMER for each substep until a kilometer step has been taken. SHAPER computes the absorption as a function of time through the pulse, making use of EVSOLVE, which generates the necessary collision rates based on the pulse rms field strength and frequency as a function of time. SUMMER integrates the attenuated pulse to obtain the fluence, propagation efficiency, and other relevant propagation parameters for graphics purposes. If propagation is upward and the target altitude is greater than 80 km, then ionospheric propagation is also computed from 80 km in much the same way as downward propagation is computed. For a monopulse, SNEAKY-II attempts to include the effects of dispersion and absorption simultaneously between 80 and 100 km. These effects are included by computing the total electron content along the propagation path and estimating the distortion of the pulse due to dispersion in SHAPER. The pulse distortion is manifested as an effective frequency that in turn enters into the calculation of the attenuation scale length.

SNEAKY-II output consists of tabulated values of the output parameters (Table II) and graphic output (Figs. 8–15). The output parameters include altitude in kilometers, maximum rms electric field in volts per centimeter, the time in seconds where the pulse amplitude has been attenuated to 0.9 of its maximum amplitude, the average power density (defined to be the integrated fluence divided by the initial pulse length), the fluence in microJoules per centimeter squared, the efficiency as defined above, and the total received power (in decibels milliwatts) to be measured by an antenna (at the target altitude) with a specified gain. These parameters are tabulated at 1-km intervals in the altitude range from 0–100 km and only at the target and/or platform altitude outside this range.

Table II
SNEAKY-II Sample Output

Altitude (km)	E Field (V/cm)	Pulse Length (s)	Power Density (W/cm^2)	Fluence ($\mu J/cm^2$)	Efficiency
0	1.121E+04	3.000E−09	3.333E+05	1.000E+03	1.000E+00
1	1.121E+04	3.000E−09	3.333E+05	1.000E+03	1.000E+00
2	1.121E+04	3.000E−09	3.333E+05	1.000E+03	1.000E+00
3	1.121E+04	3.000E−09	3.333E+05	1.000E+03	1.000E+00
4	1.121E+04	3.000E−09	3.333E+05	1.000E+03	1.000E+00
5	1.121E+04	3.000E−09	3.333E+05	1.000E+03	1.000E+00
6	1.121E+04	3.000E−09	3.333E+05	1.000E+03	1.000E+00
7	1.121E+04	3.000E−09	3.333E+05	1.000E+03	1.000E+00
8	1.121E+04	3.000E−09	3.333E+05	1.000E+03	1.000E+00
9	1.121E+04	3.000E−09	3.333E+05	1.000E+03	1.000E+00
10	1.121E+04	3.000E−09	3.333E+05	1.000E+03	1.000E+00
11	1.121E+04	3.000E−09	3.333E+05	1.000E+03	1.000E+00
12	1.121E+04	3.000E−09	3.333E+05	1.000E+03	1.000E+00
13	1.121E+04	3.000E−09	3.333E+05	1.000E+03	1.000E+00
14	1.121E+04	3.000E−09	3.333E+05	1.000E+03	1.000E+00
15	1.121E+04	3.000E−09	3.333E+05	1.000E+03	1.000E+00
16	1.121E+04	3.000E−09	3.333E+05	1.000E+03	1.000E+00
17	1.121E+04	3.000E−09	3.333E+05	9.999E+02	9.999E−01
18	1.121E+04	3.000E−09	3.326E+05	9.978E+02	9.978E−01
19	1.121E+04	2.723E−09	3.161E+05	9.483E+02	9.483E−01
20	1.121E+04	2.324E−09	2.755E+05	8.265E+02	8.265E−01
21	1.121E+04	2.034E−09	2.413E+05	7.240E+02	7.241E−01
22	1.121E+04	1.791E−09	2.126E+05	6.377E+02	6.377E−01
23	1.121E+04	1.593E−09	1.891E+05	5.674E+02	5.674E−01
24	1.121E+04	1.435E−09	1.705E+05	5.114E+02	5.115E−01
25	1.121E+04	1.309E−09	1.556E+05	4.668E+02	4.669E−01
26	1.121E+04	1.206E−09	1.435E+05	4.305E+02	4.306E−01
27	1.121E+04	1.123E−09	1.337E+05	4.012E+02	4.012E−01
28	1.121E+04	1.054E−09	1.257E+05	3.772E+02	3.772E−01
29	1.121E+04	9.992E−10	1.193E+05	3.578E+02	3.578E−01
30	1.121E+04	9.543E−10	1.140E+05	3.421E+02	3.421E−01
31	1.121E+04	9.175E−10	1.098E+05	3.293E+02	3.293E−01
32	1.121E+04	8.879E−10	1.064E+05	3.191E+02	3.191E−01
33	1.121E+04	8.639E−10	1.036E+05	3.109E+02	3.110E−01
34	1.121E+04	8.453E−10	1.016E+05	3.047E+02	3.047E−01
35	1.121E+04	8.314E−10	1.000E+05	3.001E+02	3.001E−01
36	1.121E+04	8.212E−10	9.893E+04	2.968E+02	2.968E−01
37	1.121E+04	8.138E−10	9.816E+04	2.945E+02	2.945E−01
38	1.121E+04	8.088E−10	9.764E+04	2.929E+02	2.929E−01
39	1.121E+04	8.053E−10	9.730E+04	2.919E+02	2.919E−01
40	1.121E+04	8.030E−10	9.708E+04	2.912E+02	2.912E−01
41	1.121E+04	8.016E−10	9.693E+04	2.908E+02	2.908E−01
42	1.121E+04	8.005E−10	9.684E+04	2.905E+02	2.905E−01
43	1.121E+04	7.997E−10	9.679E+04	2.904E+02	2.904E−01
44	1.121E+04	7.992E−10	9.675E+04	2.903E+02	2.903E−01
45	1.121E+04	7.989E−10	9.673E+04	2.902E+02	2.902E−01
46	1.121E+04	7.988E−10	9.672E+04	2.901E+02	2.902E−01
47	1.121E+04	7.987E−10	9.671E+04	2.901E+02	2.901E−01
48	1.121E+04	7.986E−10	9.670E+04	2.901E+02	2.901E−01

49	1.121E+04	7.986E−10	9.670E+04	2.901E+02	2.901E−01
50	1.121E+04	7.986E−10	9.668E+04	2.901E+02	2.901E−01
51	1.121E+04	7.986E−10	9.668E+04	2.900E+02	2.900E−01
52	1.121E+04	7.985E−10	9.667E+04	2.900E+02	2.901E−01
53	1.121E+04	7.985E−10	9.667E+04	2.900E+02	2.900E−01
54	1.121E+04	7.985E−10	9.667E+04	2.900E+02	2.900E−01
55	1.121E+04	7.985E−10	9.667E+04	2.900E+02	2.900E−01
56	1.121E+04	7.985E−10	9.666E+04	2.900E+02	2.900E−01
57	1.121E+04	7.985E−10	9.665E+04	2.900E+02	2.900E−01
58	1.121E+04	7.985E−10	9.665E+04	2.899E+02	2.900E−01
59	1.121E+04	7.985E−10	9.665E+04	2.899E+02	2.900E−01
60	1.121E+04	7.985E−10	9.664E+04	2.899E+02	2.899E−01
61	1.121E+04	7.985E−10	9.664E+04	2.899E+02	2.899E−01
62	1.121E+04	7.985E−10	9.664E+04	2.899E+02	2.899E−01
63	1.121E+04	7.985E−10	9.663E+04	2.899E+02	2.899E−01
64	1.121E+04	7.985E−10	9.663E+04	2.899E+02	2.899E−01
65	1.121E+04	7.985E−10	9.662E+04	2.899E+02	2.899E−01
66	1.121E+04	7.985E−10	9.661E+04	2.898E+02	2.899E−01
67	1.121E+04	7.985E−10	9.661E+04	2.898E+02	2.898E−01
68	1.121E+04	7.985E−10	9.661E+04	2.898E+02	2.898E−01
69	1.121E+04	7.985E−10	9.661E+04	2.898E+02	2.898E−01
70	1.121E+04	7.985E−10	9.660E+04	2.898E+02	2.898E−01
71	1.121E+04	7.984E−10	9.660E+04	2.898E+02	2.898E−01
72	1.121E+04	7.984E−10	9.659E+04	2.898E+02	2.898E−01
73	1.121E+04	7.984E−10	9.659E+04	2.898E+02	2.898E−01
74	1.121E+04	7.984E−10	9.658E+04	2.898E+02	2.898E−01
75	1.121E+04	7.984E−10	9.659E+04	2.898E+02	2.898E−01
76	1.121E+04	7.984E−10	9.657E+04	2.897E+02	2.897E−01
77	1.121E+04	7.984E−10	9.657E+04	2.897E+02	2.897E−01
78	1.121E+04	7.984E−10	9.657E+04	2.897E+02	2.897E−01
79	1.121E+04	7.984E−10	9.658E+04	2.897E+02	2.897E−01
80	1.121E+04	7.984E−10	9.656E+04	2.897E+02	2.897E−01
81	1.121E+04	7.984E−10	9.655E+04	2.897E+02	2.897E−01
82	1.121E+04	7.984E−10	9.655E+04	2.896E+02	2.896E−01
83	1.121E+04	7.984E−10	9.654E+04	2.896E+02	2.896E−01
84	1.121E+04	7.984E−10	9.654E+04	2.896E+02	2.896E−01
85	1.121E+04	7.984E−10	9.653E+04	2.896E+02	2.896E−01
86	1.121E+04	7.984E−10	9.652E+04	2.896E+02	2.896E−01
87	1.121E+04	7.984E−10	9.652E+04	2.896E+02	2.896E−01
88	1.121E+04	7.984E−10	9.651E+04	2.895E+02	2.895E−01
89	1.121E+04	7.984E−10	9.651E+04	2.895E+02	2.895E−01
90	1.121E+04	7.984E−10	9.651E+04	2.895E+02	2.895E−01
91	1.121E+04	7.984E−10	9.649E+04	2.895E+02	2.895E−01
92	1.121E+04	7.984E−10	9.649E+04	2.895E+02	2.895E−01
93	1.121E+04	7.984E−10	9.648E+04	2.895E+02	2.895E−01
94	1.121E+04	7.984E−10	9.648E+04	2.894E+02	2.895E−01
95	1.121E+04	7.984E−10	9.647E+04	2.894E+02	2.895E−01
96	1.121E+04	7.984E−10	9.646E+04	2.894E+02	2.895E−01
97	1.121E+04	7.984E−10	9.646E+04	2.894E+02	2.895E−01
98	1.121E+04	7.984E−10	9.645E+04	2.893E+02	2.895E−01
99	1.121E+04	7.984E−10	9.644E+04	2.893E+02	2.895E−01
100	1.121E+04	7.984E−10	9.643E+04	2.893E+02	2.895E−01

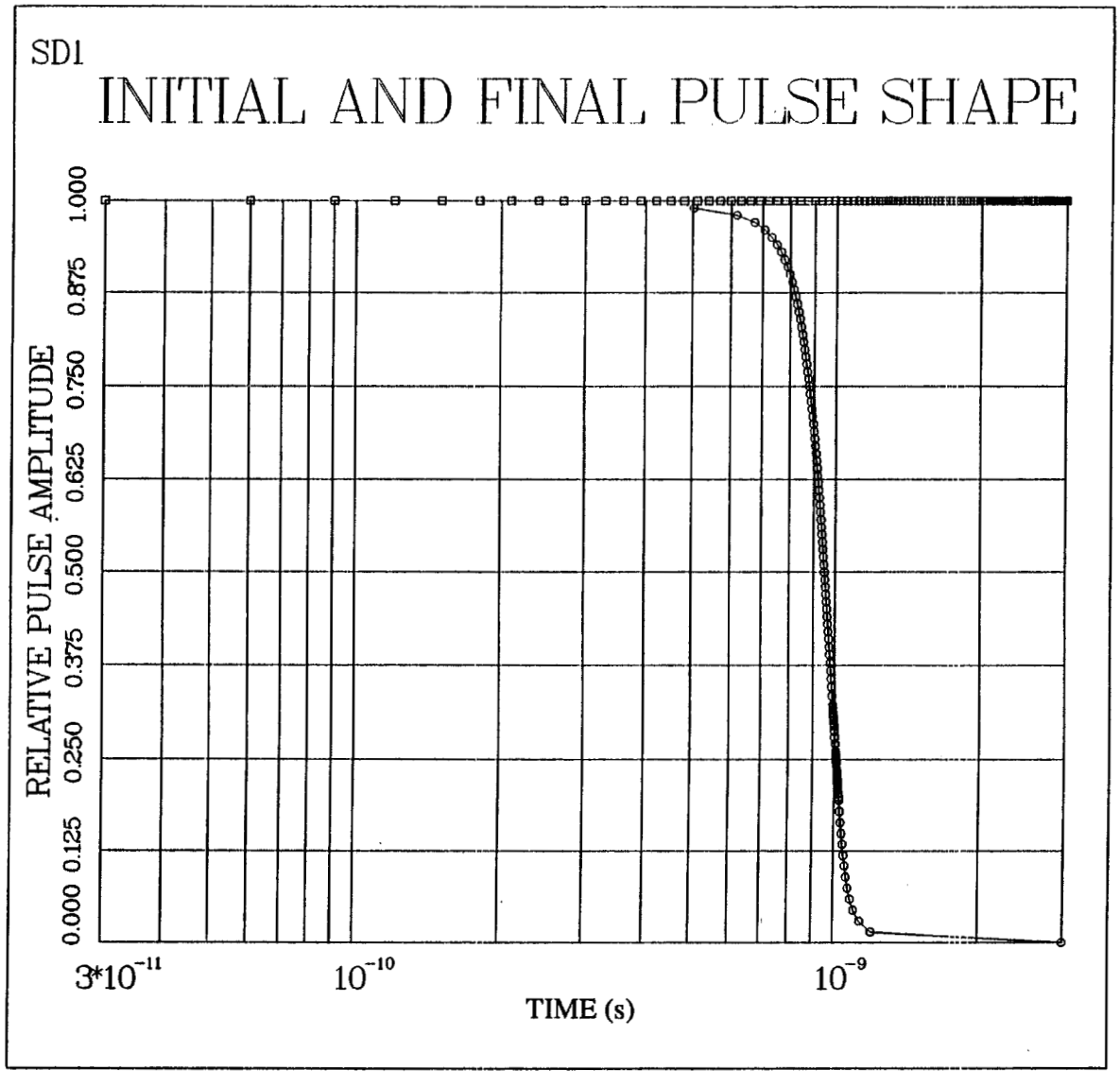

Fig. 8. The initial and final normalized pulse shapes are plotted vs time on a linear scale.

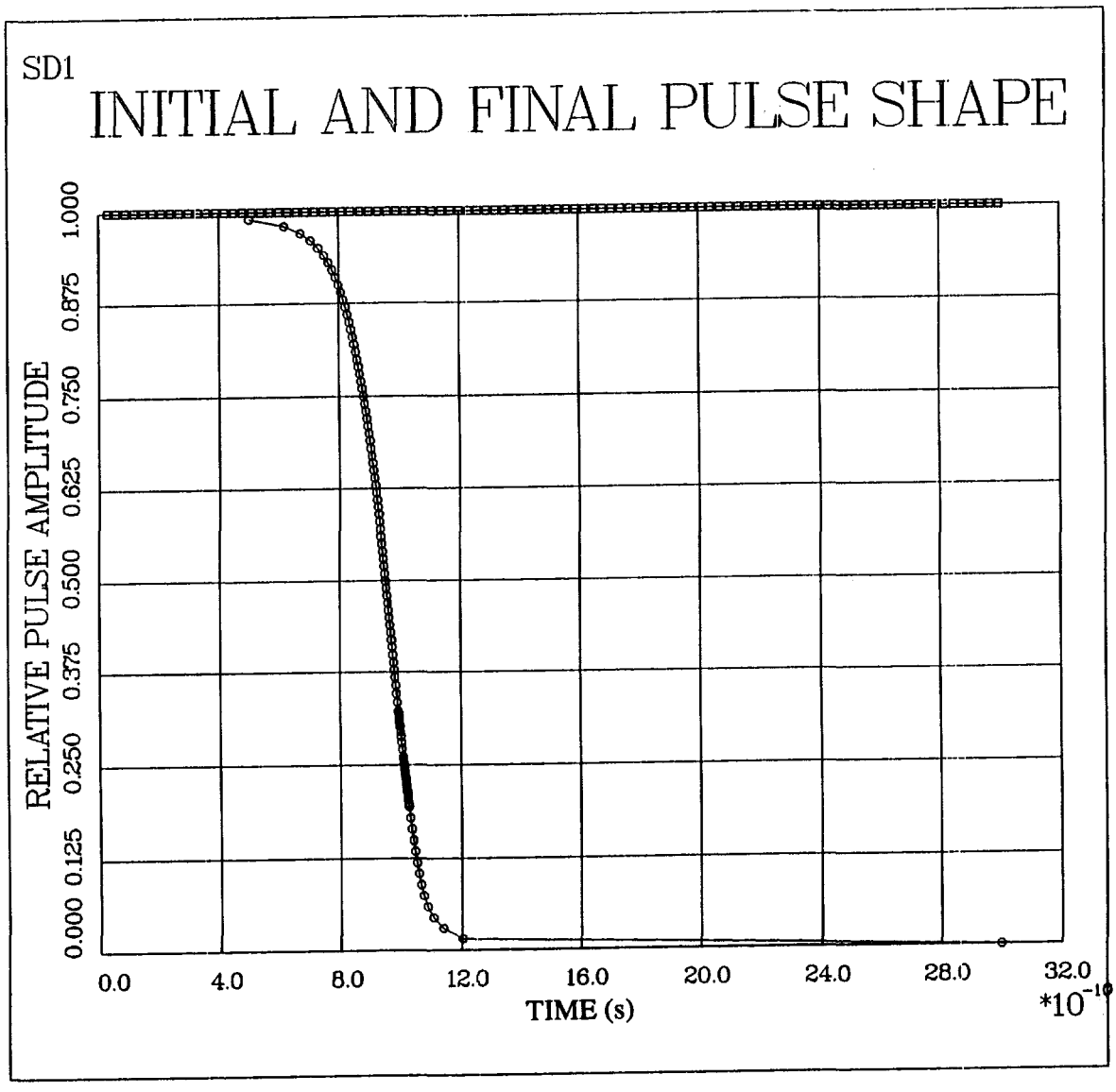

Fig. 9. The initial and final normalized pulse shapes are plotted vs time on a log scale.

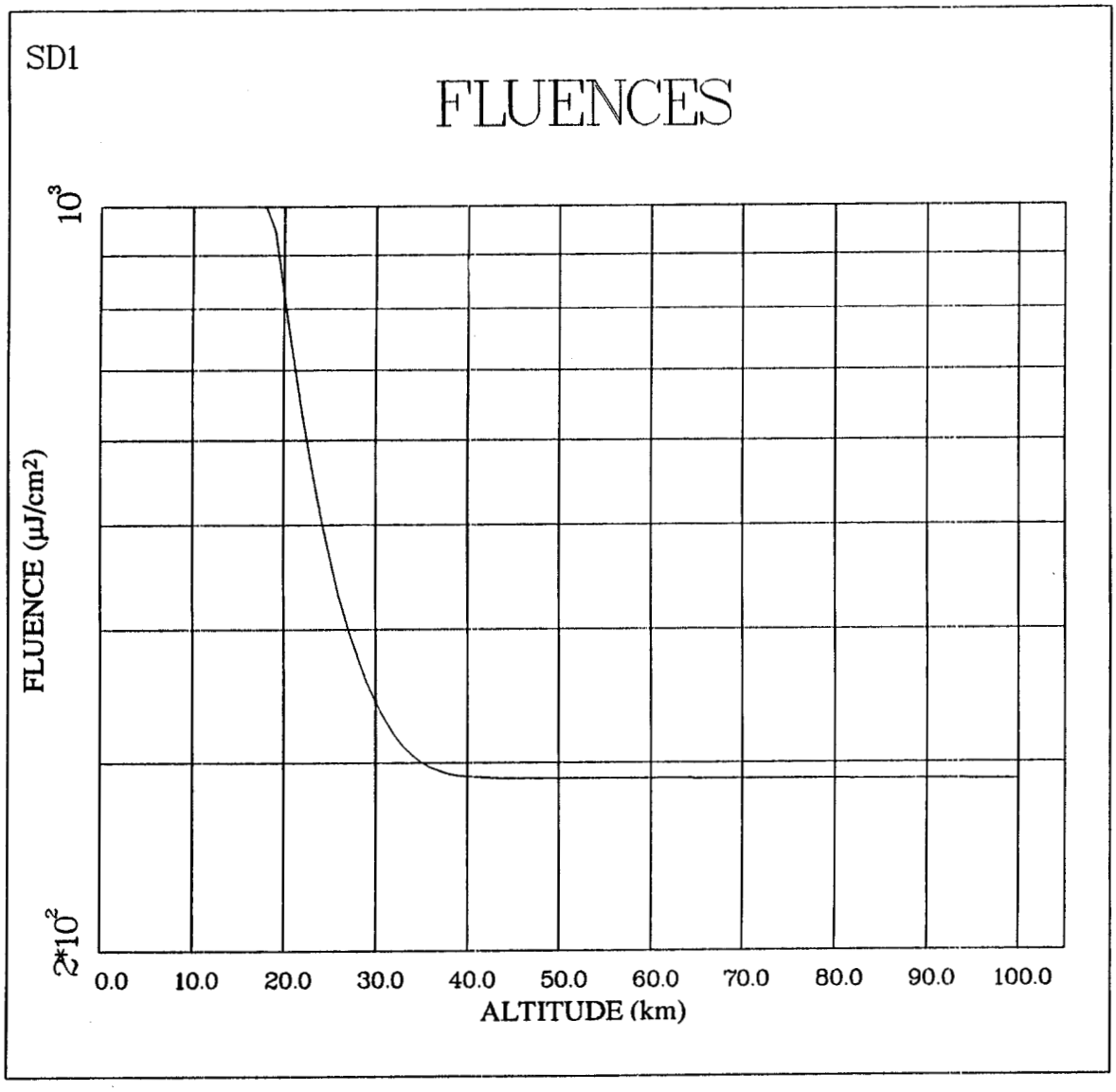

Fig. 10. The microwave fluence is plotted vs altitude.

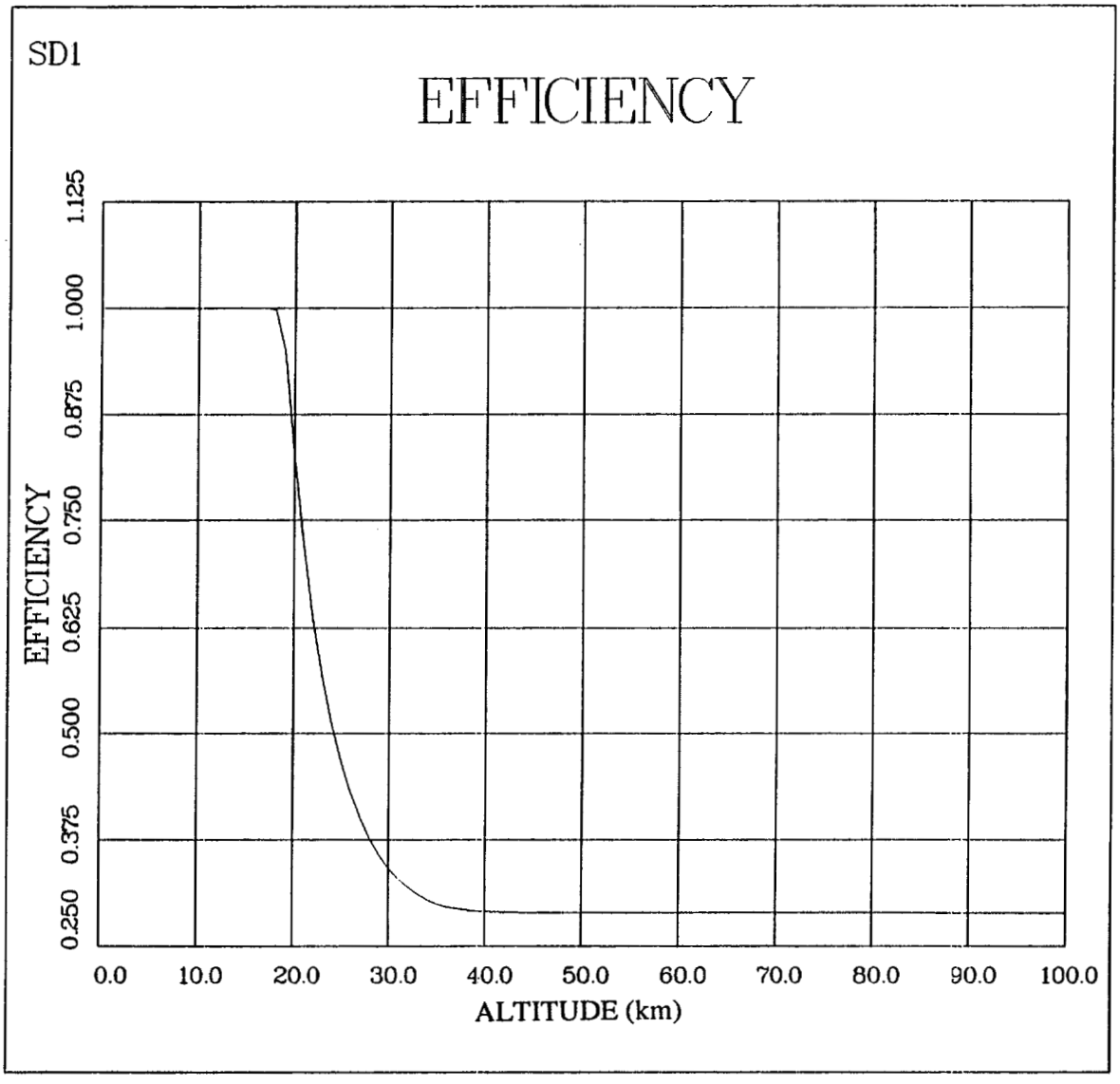

Fig. 11. The efficiency defined to be the total energy at a given altitude divided by the initial total energy is plotted vs altitude.

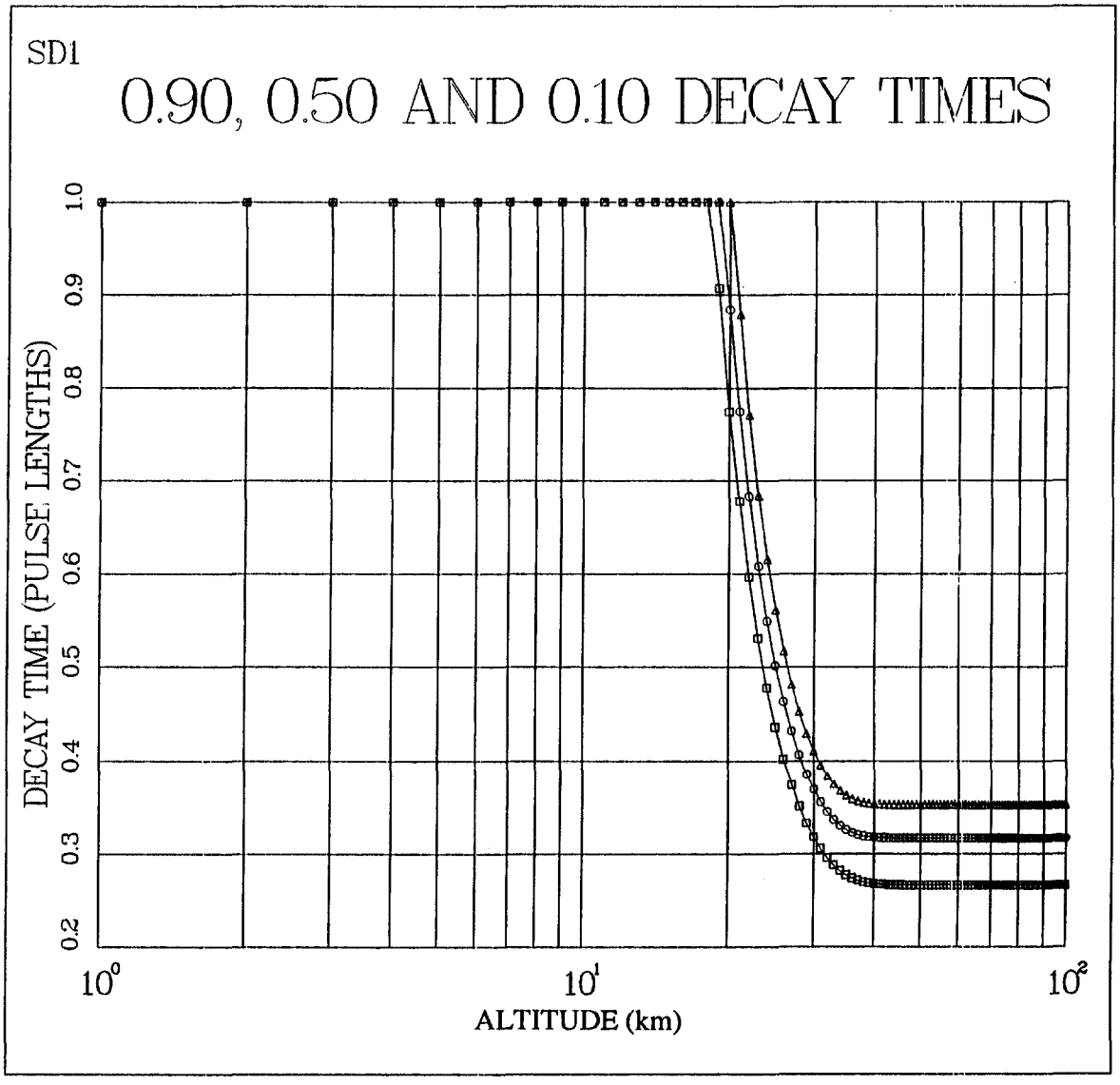

Fig. 12. Times corresponding to normalized pulse amplitudes of 0.9 (□), 0.5 (○), and 0.1 (△) are plotted as a function of altitude.

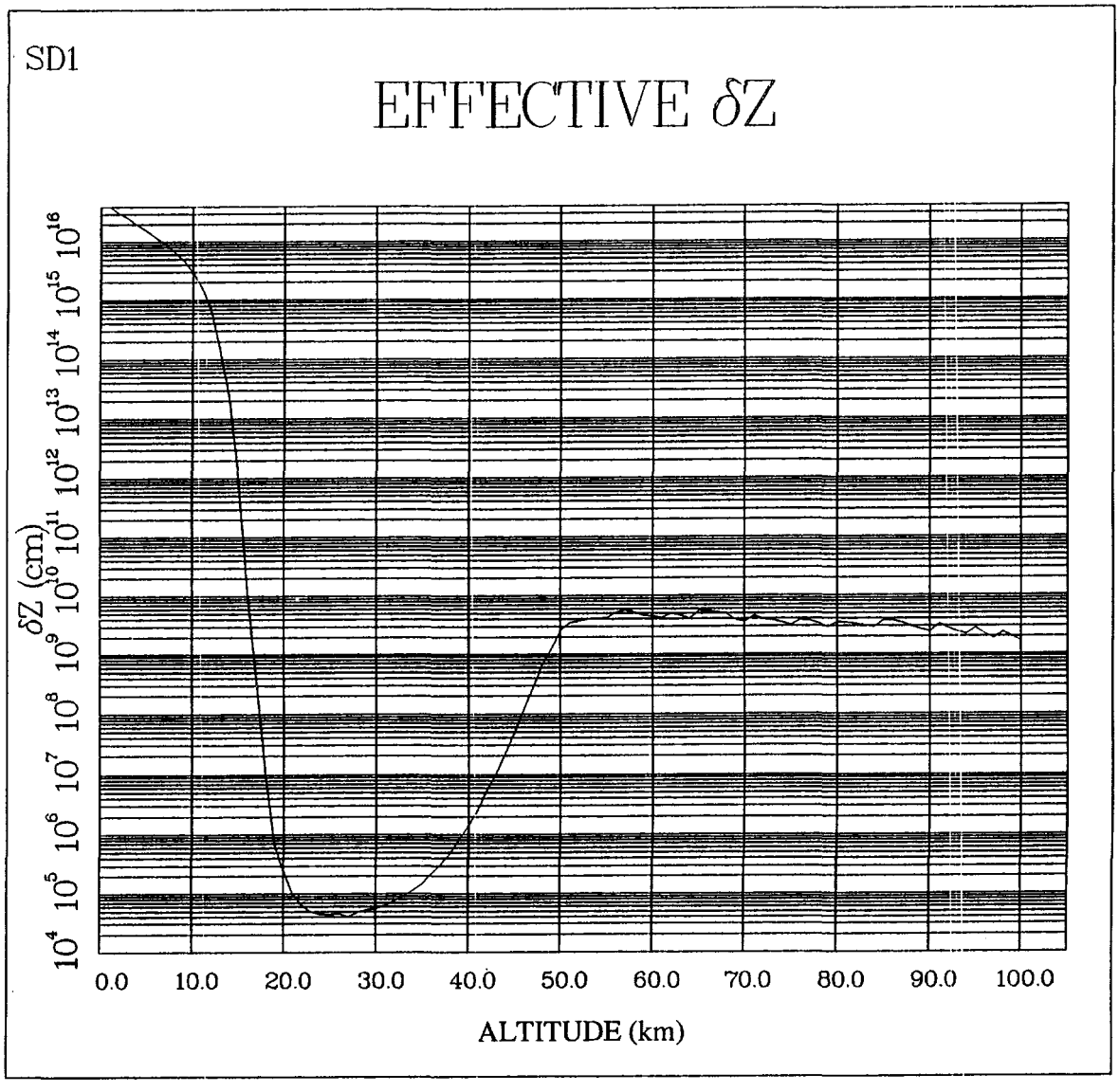

Fig. 13. The effective attenuation scale length defined in Section III.F is plotted as a function of altitude.

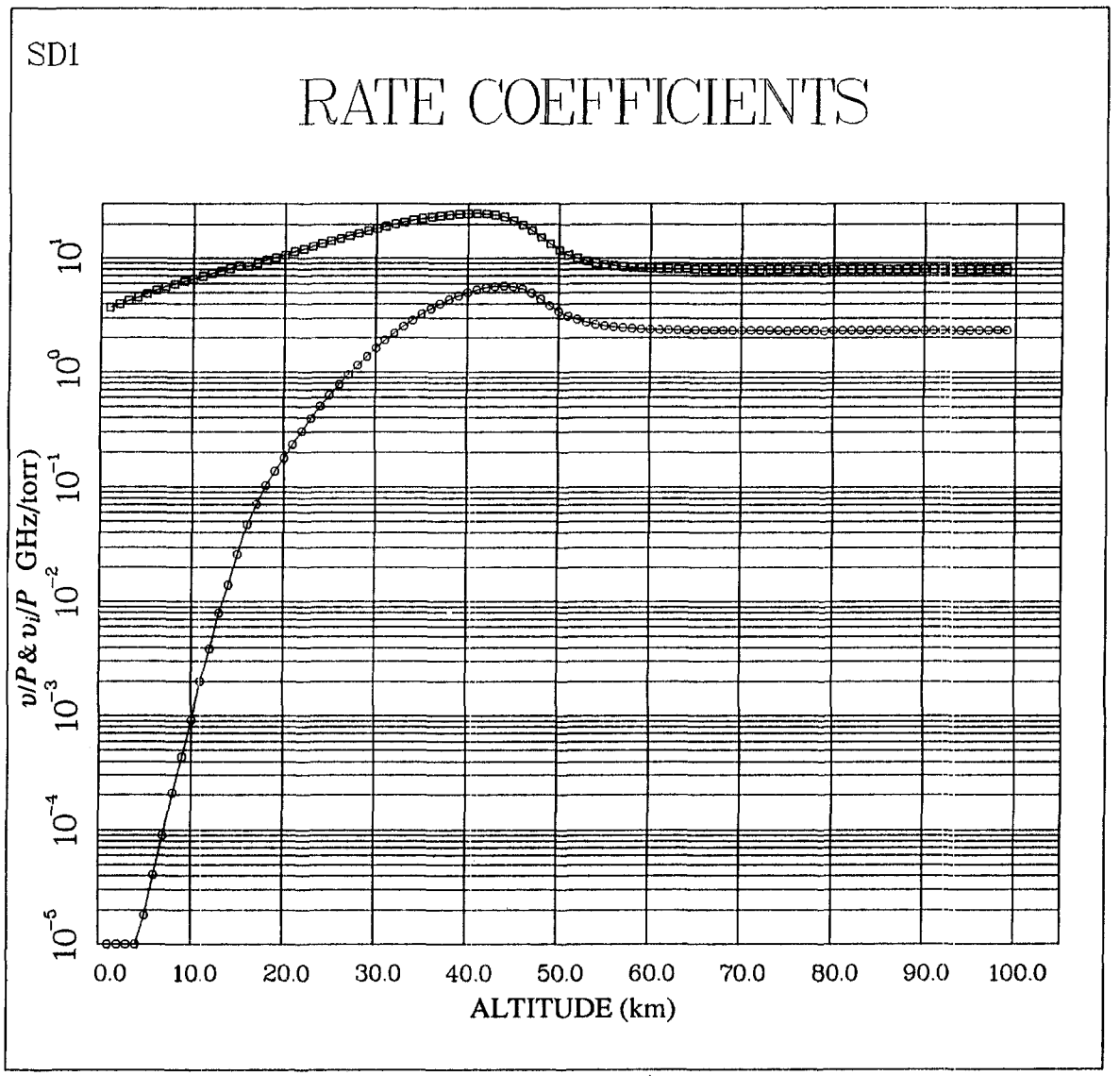

Fig. 14. The ionization and momentum exchange rates averaged over the pulse are plotted as a function of altitude.

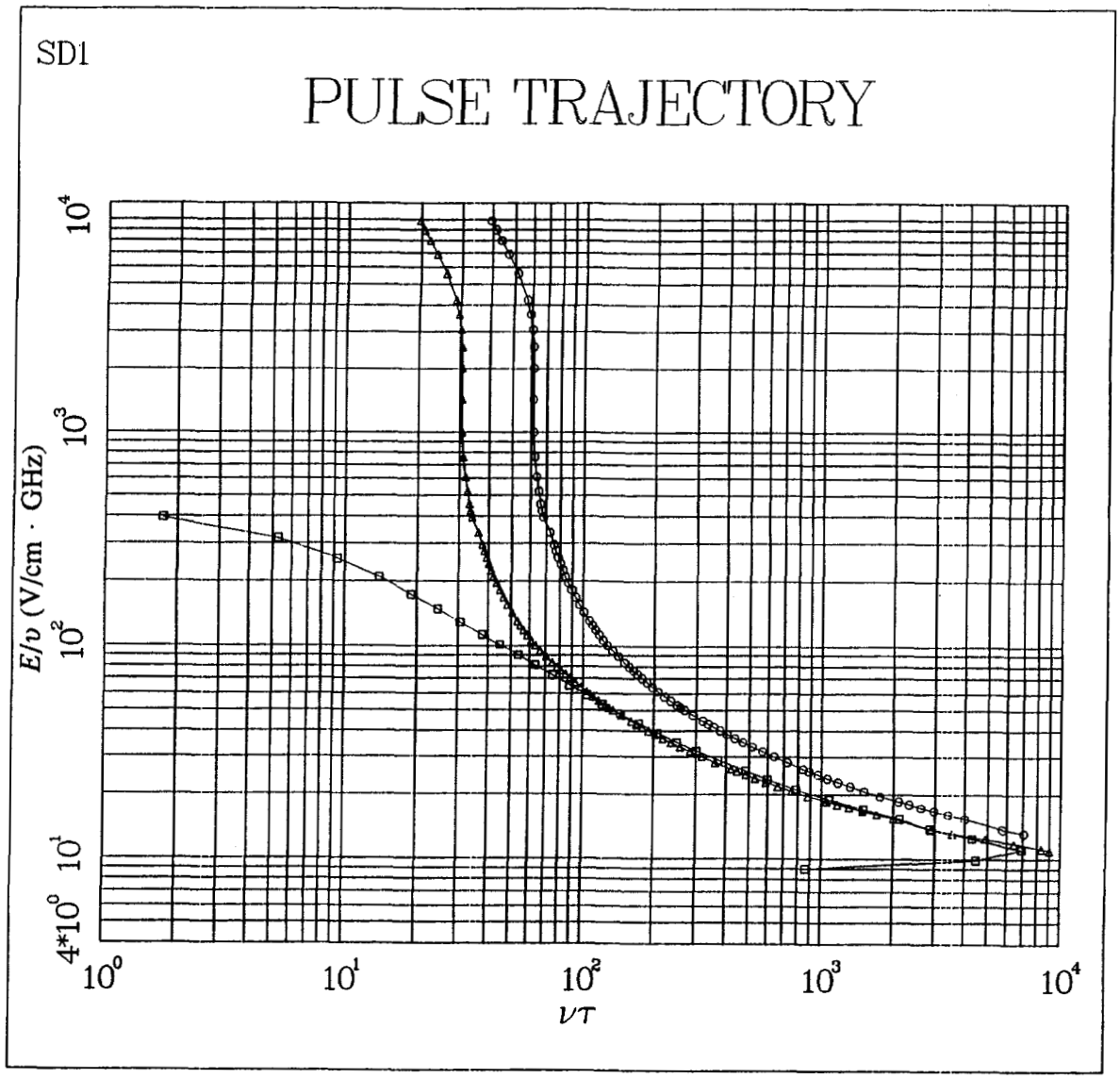

Fig. 15. Breakdown thresholds (○), tail-erosion thresholds based on 1-km attenuation scale length (△), and the pulse trajectory (□) are plotted in the E_{eff}/ν vs $\nu\tau$ space (see Section III.F).

The graphic output consists of 8–14 plots, depending on whether or not transionospheric propagation is performed. In order, these plots include 1) the initial and final normalized profile functions $[u(n,t)]$ vs time on a linear scale; 2) same as 1) but on a log-time scale; 3) fluence vs altitude; 4) efficiency vs altitude; 5) the 0.9, 0.5, and 0.1 decay times vs altitude; 6) an effective attenuation scale length (see Section III.F) vs altitude; 7) ionization and momentum exchange rates vs altitude; and 8) the pulse trajectory in E_{eff}/v vs $v\tau$ space.

V. BENCHMARKING

A. SNEAKY-II vs Fluid Calculations

The accuracy of the SNEAKY-II code in predicting delivered fluence, propagation efficiency (or atmospheric transmission), and final pulse shape was checked against detailed fluid calculations for a broad range of scenarios. Antenna parameters were chosen to cover a range of divergence angles and antenna diameters. Pulse lengths were varied from nanoseconds to microseconds while frequencies of 0, 1, and 3 GHz (where $f = 0$ refers to a monopulse) were studied. Both codes were run for several values for the total energy in the pulse and several pulse shapes. The results are summarized in Table III.

Cases 1–8 in Table III are characterized by a constant total energy (E_{tot}), two sets of antenna parameters (R = antenna radius and θ = divergence angle), microwave frequencies (f) of 1 and 3 GHz, and pulse lengths (τ) ranging from 2 to 1000 ns. Vertical propagation was carried out in each of these cases from a platform altitude of 100 km to a target altitude on the ground. The computed fluences and efficiencies on the ground show a 1%–13% range of discrepancies between FLAP and SNEAKY-II. For cases 9–19 antenna divergence was omitted (i.e., plane-wave propagation was assumed), the total energy was varied from 0.02 to 70 J, and pulse lengths ranging from 1 to 1000 ns and microwave frequencies of 1 and 3 GHz as well as a monopulse were treated. Propagation was carried out from 0 to 100 km for all cases except 18 and 19, where propagation was stopped at 60 and 70 km, respectively (altitudes above which relativistic effects become important). For these cases the computed fluences and efficiencies show a range of discrepancies between FLAP and SNEAKY-II of from 1%–13%.

If we consider the number of parameters and potential range of values for each, the number of benchmark cases is rather limited. Nevertheless, a representative sample of values as well as a few extremes was chosen for each parameter. Although we fully expect the range of discrepancy to remain at 1%–13%, we recommend that spot checks against FLAP be made in future parameter studies performed with SNEAKY-II.

B. Fluid vs Experiment

The absolute accuracy of the fluid code (FLAP) was tested by comparing breakdown thresholds against the experimental results of Felsenthal and Proud (1962) and those of Byrne (1986). As noted above, breakdown can be defined as the time for the electron swarm to avalanche in the presence of a given electric field to a specified density. In the fluid calculations we obtain the time τ that it takes the electron density to reach a value 10^8 times larger than its initial value (a formulation adopted by Felsenthal and Proud) from the avalanche rate calculated for a specified value of electric field strength to neutral pressure (E/P). In this way a plot of E/P vs $P\tau$ can be generated for comparison with experimental results. Figure 16 shows such a plot comparing fluid calculations with

Table III
Benchmark Results for SNEAKY-II vs FLAP[a]

						FLAP		SNEAKY-II	
Case	R (m)	θ (°)	E_{tot} (J)	τ (ns)	f (GHz)	F_ℓ (μJ/cm^2)	E	F_ℓ (μJ/cm^2)	E
1	17300	19	10^{10}	3	1	63.4	0.50	63.5	0.54
2	17300	19	10^{10}	2	3	89.4	0.70	86.2	0.73
3	5500	5.7	10^{10}	3	1	275	0.21	283.	0.21
4	5500	5.7	10^{10}	2	3	369	0.28	363.	0.28
5	17300	19	10^{10}	6	1	39.8	0.31	41.1	0.35
6	5500	5.7	10^{10}	6	1	167	0.13	186.	0.14
7	5500	5.7	10^{10}	100	1	28.7	0.022	32.3	0.024
8	5500	5.7	10^{10}	1000	1	7.73	0.0059	8.47	0.0064
9	0.56	181	10	3	1	319	31.9	289	28.9
10	0.56	181	20	10	1	226	11.3	214	10.7
11	0.56	181	4.0	30	1	42.7	10.7	42.1	10.5
12	0.56	181	2.5	100	1	16.9	6.75	17.3	7.3
13	0.56	181	1.0	1000	1	9.39	9.39	10.6	10.6
14	0.56	181	30.	1	3	1091.	36.4	1032	34.4
15	0.56	181	70.	3	3	952.	13.6	894	12.8
16	0.56	181	10.	10	3	141.	14.1	148	14.8
17	0.56	181	0.020	2.3	0	1.02	50.8	1.02	50.8
18	0.56	181	6.0	3	0	183	30.5	189	31.5
19	0.56	181	9.0	10	0	75.3	8.35	71.4	7.94

[a] The parameters in this table are defined as follows: R is the antenna radius in meters; θ is the angular divergence (half-angle) of the radiation from the antenna in degrees; E_{tot} is the total energy in the microwave pulse in Joules; τ is the total length of the pulse in nanoseconds; f is the central frequency of the pulse in GHz; F_ℓ is the fluence calculated to reach the target in microJoules per centimeter squared; and E is the propagation efficiency, i.e., the total energy reaching the target divided by the total energy radiated at the antenna.

the measured dc results of Felsenthal and Proud. The agreement with data is within 30% in the range $2 \times 10^{-7} < P\tau < 2 \times 10^{-5}$ and $3 \times 10^{-9} < P\tau < 7 \times 10^{-9}$. Outside this range, the agreement is less satisfactory. At high pressure we see the effect of the high-energy tail, as the fluid calculations can underestimate the avalanche rates by orders of magnitude. At low pressure we find the fluid calculations underestimate these rates by factors of two, a result that could be explained in terms of nonequilibrium effects.

A similar study was performed for microwave pulses. The fluid calculations for breakdown thresholds in this case are plotted in terms of an effective breakdown field, defined by Eq. (3) with the momentum collision frequency approximated as $\nu = 5.3 \times 10^9\ P$. Results of our calculations are compared against the recent S-band measurements of Byrne shown in Fig. 17. Again the agreement is excellent for intermediate values of $P\tau$, while strong discrepancies exist at low and high pressures as in the dc calculations. These results underscore the need to incorporate experimental measurements of collision rates into the SNEAKY-II tables and to pursue more detailed kinetic calculations of breakdown and propagation.

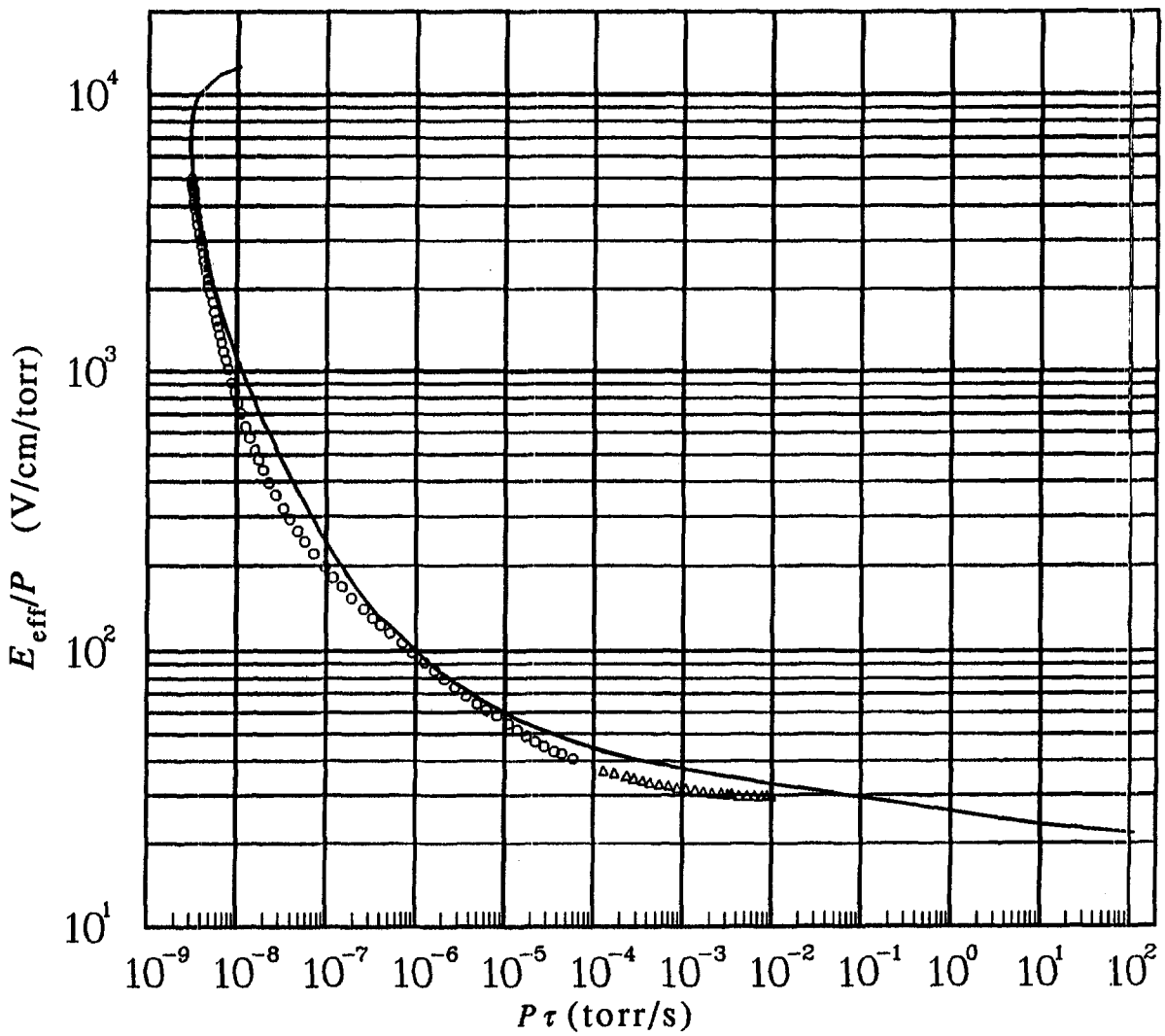

Fig. 16. Comparison of fluid calculations for breakdown thresholds vs the experimental dc results of Felsenthal and Proud ○ and Gould and Roberts (△).

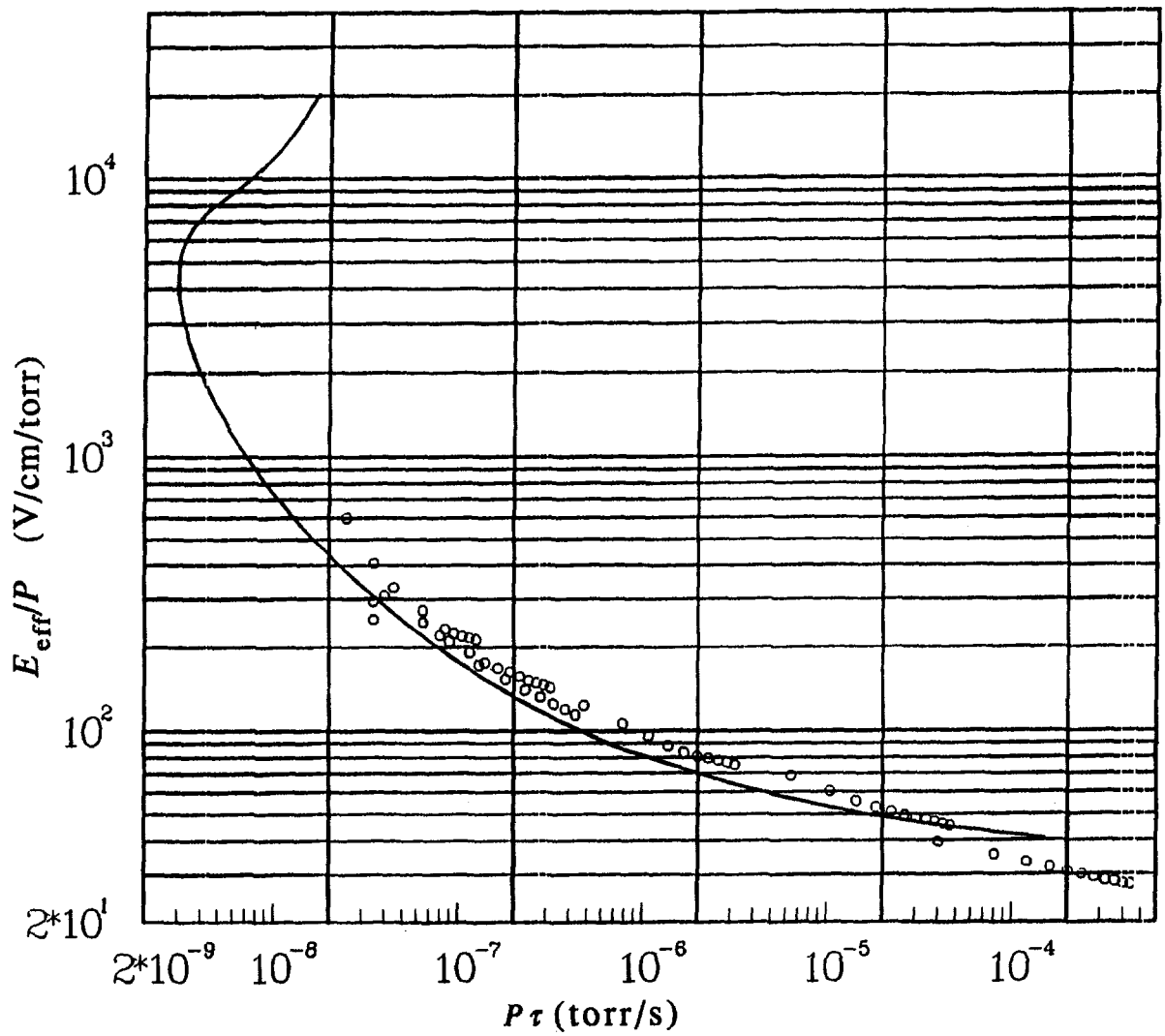

Fig. 17. Comparison of fluid calculations for HPM breakdown thresholds against the recent S-band measurements of Byrne (O).

VI. SUMMARY AND FUTURE WORK

A. Summary

The SNEAKY-II code is an enormously useful tool in providing quick and accurate estimates of air transmission to high-power microwaves. The benchmark calculations performed against a more detailed fluid treatment provide an estimate of expected errors for transmitted fluence and transmission efficiency in the 1%–13% range for a broad range of propagation parameters. These results verify the scaling laws that form the basis of the SNEAKY algorithm and suggest that measured rates can be used to insure absolute accuracy to within experimental errors. It is anticipated that this code will play an important role as part of a larger system code designed to assess the potential threat of HPM devices.

At the same time SNEAKY-II possesses certain limitations. First, it treats only the problems of self-absorption caused by air breakdown and dispersion and does not include the effects of gaseous absorption or scattering in the presence of rain drops or ice particles, effects that become important above approximately 10 GHz. In addition the treatment of air breakdown assumes that a uniform distribution of seed electrons is available to initiate the avalanching process, a condition that does not prevail at sea level where the statistics of cosmic-ray ionization determines the electron population. At present SNEAKY-II does not include realistic antenna profiles, does not treat two-dimensional effects, and is limited to the nonrelativistic regime. The basic framework of the code, however, is such that many of these effects can be incorporated.

B. Future Work

It is important that SNEAKY-II be kept current with any new breakdown and/or electron transport data as well as with any advancements in the area of HPM propagation. Some issues of current interest include 1) a two-dimensional analysis of statistical breakdown at sea level; 2) inclusion of relativistic effects to treat low-pressure, high-power propagation; and 3) treatment of propagation through a highly ionized and structured environment. In addition, in attempting to optimize air transmission, it is conceivable that special pulse shapes will be of interest (e.g., chirped pulses). In addition, it is possible that specific physical effects such as self-focusing would become attractive for particular applications. Each of these could be addressed as future needs are identified.

ACKNOWLEDGMENTS

We would like to acknowledge the efforts of Maj. David Ellis (FCDNA), Capt. Ray Jellerson (AFWL), and Capt. Dean Oyler (AFWL) in developing an initial coded version of SNEAKY from which the significantly enhanced SNEAKY-II was later conceived and written. This work was performed under the auspices of the US Department of Energy and the US Department of Defense.

REFERENCES

Byrne, D. P., 1986, "Intense Microwave Pulse Propagation Through Gas Breakdown Plasmas in a Waveguide," UCRL-53764, Ph.D. thesis, Lawrence Livermore National Laboratory, p. 159.

Felsenthal, P., and J. M. Proud, 1965, *Phys. Rev.*, **139**, No. 6A, A1796.

Felsenthal, P., 1966, *J. Appl. Phys.*, **37**, No. 12, 4557.

Gould, L., and L. W. Roberts, 1956, *J. Appl. Phys.*, 27, 1162.

Roussel-Dupre, R. A., and T. Tunnell, 1989, "High-Power Microwave Propagation in Air. I. Fluid Treatment," in preparation.

☆U.S. GOVERNMENT PRINTING OFFICE: 1989-773-034/00245

Page Range	NTIS Price Code	Page Range	NTIS Price Code	Page Range	NTIS Price Code	Page Range	NTIS Price Code
001–025	A02	151–175	A08	301–325	A14	451–475	A20
026–050	A03	176–200	A09	326–350	A15	476–500	A21
051–075	A04	201–225	A10	351–375	A16	501–525	A22
076–100	A05	226–250	A11	376–400	A17	526–550	A23
101–125	A06	251–275	A12	401–425	A18	551–575	A24
126–150	A07	276–300	A13	426–450	A19	576–600	A25
						601-up*	A99

*Contact NTIS for a price quote.

Los Alamos Los Alamos National Laboratory
Los Alamos,New Mexico 87545